Traitor-virus-guided discovery of novel antiviral factors

Caterina Prelli Bozzo[1#], Alexandre Laliberté[1#], Aurora De Luna[1], Chiara Pastorio[1], Kerstin Regensburger[1], Stefan Krebs[2], Alexander Graf[2], Helmut Blum[2], Meta Volcic[1], Konstantin M.J. Sparrer[1*] & Frank Kirchhoff[1*]

[1] Institute of Molecular Virology
Ulm University Medical Center
89081 Ulm, Germany

[2] Laboratory for Functional Genome Analysis
Gene Center, LMU Munich,
81377 Munich, Germany

[#]both contributed equally

*Correspondence: Konstantin.Sparrer@uni-ulm.de and Frank.Kirchhoff@uni-ulm.de

Keywords: HIV-1, restriction factors, CRISPR/Cas9, interferon, replication-competent HIV-1 gRNA constructs, Granulin, MHC-II Complex Transactivator, IFI16

Abstract

Complex pathogen-host interactions govern the outcome of viral exposures but remain poorly understood because current methods to elucidate antiviral mechanisms are prone to artefacts and lack sensitivity. Here, we developed a virus-guided technology platform where the pathogen itself reveals its cellular opponents. To accomplish this, we engineered replication-competent HIV-1 expressing sgRNAs targeting potential antiviral genes in Cas9-expressing $CD4^+$ T cells. Simultaneous analysis of HIV-1 constructs targeting >500 candidate genes revealed that sgRNAs against *GRN*, *CIITA*, *EHMT2*, *CEACAM3*, *CC2D1B*, *RHOA* and *HMOX1* are strongly enriched over several rounds of replication. Overexpression and knock-out studies confirmed the antiretroviral activity of most factors but failed for some. Finally, we show that lack of the accessory *nef* gene increased enrichment of sgRNAs targeting SERINC5 and IFI16 demonstrating that this method allows identification of targets of accessory proteins. The versatile and effective HIV-guided CRISPR technology offers numerous possibilities for clarification of virus-host interactions and innate defense mechanisms.

Introduction

Viral pathogens and their hosts are caught in an ever-ongoing arms race. Cellular antiviral factors are an essential part of the innate immune system and may provide immediate and broad protection against viral pathogens[1–3]. However, viruses adapt and have evolved sophisticated mechanisms to evade or counteract antiviral defense mechanisms[4–6]. Thus, the outcome of viral exposures depends on complex pathogen-host interactions and failure of cellular defense mechanisms may result in severe disease and - in the worst case - devastating pandemics.

HIV-1 is the causative agent of the AIDS pandemic and a serious challenge to public health since more than 40 years. Studies of HIV-1 and related lentiviruses allowed the discovery of a complex repertoire of restriction factors that have the potential to inhibit viral pathogens at essentially every of their replication cycle[1–3]. They further revealed that differences in the ability to counteract antiviral restriction factors explain why only one of at least thirteen independent zoonotic lentiviral transmissions resulted in the AIDS pandemic[6–8]. However, we are only beginning to understand the complex interplay between HIV and its human host and it is evident that important antiviral factors remain to be discovered. For example, the determinants of interferon (IFN) resistance of transmitted/founder (TF) HIV-1 strains that are responsible for primary infection[9,10], frequently map to regions in the viral genome unlikely to affect the susceptibility to known restriction factors. Previous studies further suggest that targets of the HIV-1 accessory Vif, Vpu, Vpr and Nef proteins which counteract major antiviral factors remain to be identified[11,12].

The discovery of yet unknown anti-retroviral factors is of broad interest and relevance as they not only restrict HIV-1 but a wide range of viral pathogens and frequently also play roles in inflammation and cancers[13–21]. Thus, new insights into antiviral defense mechanisms will not only improve our ability to combat viral pathogens but also help to develop innovative therapies against other diseases. However, discovery of restriction factors is a challenging task since they are structurally and functionally highly diverse and there are no generally applicable

criteria for their identification[2,4]. Previous studies used expression libraries of IFN-stimulated genes (ISGs), RNA interference, and pooled CRISPR/Cas9 screens[22]. However, over-expression screens can usually not be performed genome-wide and are prone to artifacts[22–24]. RNAi screens show low reproducibility and high rates of false positives due to inefficient knock-down and off-target effects[22,25]. Most CRISPR/Cas9-based screens involve the introduction of pooled sgRNAs into Cas9-expressing cells primarily via lentiviral transduction[22] already altering the innate immune landscape of the transduced cell prior to virus infection. Subsequently, cells showing resistance or increased sensitivity in single-round virus infection assays are enriched to identify pro- or antiviral factors, respectively. So far just a single targeted CRISPR-based screen for HIV restriction factors has been reported[26]. In this approach THP-1 cells are first treated with LTR-containing constructs coexpressing Cas9 and sgRNAs, subsequently infected with wild-type HIV-1, and examined for enrichment of gRNAs in the viral supernatant compared to the cellular extracts[26]. Thus, this system uses traditional double-transductions with non-replication competent vectors and specifically detects antiviral factors associated with reduced levels of viral RNA genomes relative to the proviral DNA copy numbers in the cells.

Previous genetic screens provided some insights into virus-host interactions. However, they have significant limitations. Most of them rely on manipulation of the cells prior to virus infection. Thus, they will miss factors important for cell survival. In addition, they may yield misleading results because some cellular proteins have different effects in uninfected and infected cells. For example, viral receptors are essential for viral entry but may impair virus release and infectivity. Importantly, current overexpression, RNA interference, and CRISPR/Cas9 screens usually involve only single-cycle infections. Thus, they frequently detect factors affecting early steps of the viral replication cycle and are generally not very sensitive. Since cells exert numerous defense mechanisms the contribution of individual factors to the control of viral pathogens may seem small. However, a 2-fold growth advantage may

result in >1000-fold higher virus yields after just 10 rounds of replication. Thus, effects missed in single round of infection screens can have major impacts on viral spread *in vivo*. Altogether, robust, sensitive, broad and versatile screens that are not prone to artifacts are urgently needed for a better understanding of the complex host-pathogen interplay.

To address this, we combined the CRISPR/Cas9 technology with the selection power of replication-competent HIV-1. Specifically, we equipped full-length infectious molecular clones (IMCs) of HIV-1 with molecular tools (i.e. sgRNAs) allowing the virus to eliminate antiviral genes but at the same time revealing their identity. We named this technique the traitor virus (TV) approach since the pathogen itself identifies its cellular opponents. Our results demonstrate that TVs targeting specific antiviral genes show increased replication fitness in Cas9 expressing T cells and are rapidly enriched in emerging viral populations. We obtained first insights into the underlying mechanisms and confirmed the antiviral effect of several factors in primary human CD4+ T cells. Finally, utilization of "handicapped" *nef*-defective TVs allowed the discovery of IFI16 as a novel target of the viral accessory protein Nef. In summary, we show that the TV-guided technology allows the robust and effective identification of antiviral cellular factors including new targets of the HIV-1 accessory proteins providing in-depth insights into virus-host interactions.

Results

Design and proof-of-principle of the TV approach

To allow efficient virus-driven discovery of antiviral cellular genes, we generated replication-competent HIV-1 constructs encoding single guide RNAs (sgRNAs). Our goal was to equip HIV-1 with sequence and target-specific genetic "scissors" to generate "traitor viruses" (TVs) whose replication fitness reveals their cellular opponents. To achieve this, we inserted a cassette encompassing the human U6 promoter, sgRNAs comprised of the flexible targeting region, and an invariant scaffold into the proviral genome of the well-characterized HIV-1 NL4-3 infectious molecular clone (IMC) (Fig. 1a). The resulting proviral HIV-1 constructs express all viral genes under the control of the LTR promoter and via the regular splice sites. However, proviral integration into the host genome initiates U6-driven expression of sgRNAs and editing of their target genes in the presence of Cas9. Thus, similar to having additional accessory genes, the virus itself drives countermeasures against cellular defense mechanisms. The sgRNA expression cassette encompasses only ~351 nucleotides and hence increased the size of the viral RNA genome that is packaged into HIV-1 particles only moderately from 9833 to 10184 base-pairs. We hypothesized that this insertion should be well tolerated and enhance the replication fitness of TV variants expressing sgRNAs inactivating cellular genes that suppress steps in the viral replication cycle after proviral integration or reduce the infectiousness of progeny HIV-1 particles.

To determine whether this novel approach works in principle, we generated TV constructs encoding non-targeting (NT) control gRNAs and four unique sgRNAs targeting two established restriction factors: tetherin that inhibits virion release[27,28] and GBP5, which impairs viral infectivity by suppressing furin-mediated processing of envelope glycoproteins (Fig. 1b) [29,30]. For passaging, we generated CEM-M7 cells stably expressing Cas9. This T/B hybrid cell line expresses CD4, CCR5 and CXCR4 and contains the *GFP* reporter gene under the control of the HIV-1 LTR[31]. Since many antiviral factors including tetherin and GBP5 are IFN-

inducible, infections were performed in the absence and presence of IFN-β. Viral supernatants were collected at different days post-infection and the abundance of sgRNAs in the viral genomes determined by qRT-PCR. We observed efficient viral replication and enrichment of TVs expressing sgRNAs targeting genes encoding the restriction factors (Fig. 1b). FACS analyses confirmed that the selected HIV-1 U6-gRNA-scaffold constructs reduced tetherin and GBP5 expression by 70% and 40%, respectively (Fig. 1c). Altogether, these results provided proof-of-concept that replication-competent HIV-1 TV constructs allow effective selection of sgRNAs targeting antiviral genes.

Generation and optimization of HIV-1 U6-gRNA-scaffold libraries

To identify novel antiviral restriction factors, we generated a library of TV constructs targeting genes encoding 511 different candidate restriction factors (CRFs; Supplementary Table 1) each by three unique sgRNAs. Target genes were chosen because they share features of known restriction factors[24], or were suggested to play roles in HIV infection[32]. As controls, we used eleven non-targeting sgRNAs. The sequences of the sgRNAs were selected from the GeCKO V2 library[33] with the lowest off target scores and targeting various exons of their respective target gene. Cloning into the proviral HIV-1 NL4-3 constructs was highly efficient and measurements of colony forming units indicated an average coverage of ~1.000 individual transformants per sgRNA. Transfection of the proviral TV-NL4-3-CRF-gRNA library yielded high levels of infectious HIV-1 ($TCID_{50}$ of $7.34x10^6$ per ml virus stock) that replicated efficiently in CEM-M7 Cas9 cells. However, the quality of sequence reads rapidly declined and PCR analyses confirmed loss of the U6-gRNA-scaffold cassette in most replicating HIV-1 variants during passage (Extended Data Fig. 1a). Sequence analyses revealed that deletions were mediated by recombination of repeats flanking the U6-gRNA-scaffold sequence (Extended Data Figs.1a, 1b). Specifically, the accessory *nef* gene overlaps the U3 region of the 3′ LTR and contains *cis*-acting elements, i.e. a T-rich region, polypurine tract (PPT) and

attachment (*att*) sequences, required for reverse transcription and integration. The initial TV constructs contain these sequences, referred to as TPI-region hereafter, in both *nef* and at the beginning of the 3'LTR. To remove repetitive hotspots for recombination, we introduced 16 synonymous nucleotide changes in the *nef* open reading frame (Extended Data Fig. 1b). In addition, we mutated the 3`end of the *nef* gene representing a 2nd less prominent site for recombination. The optimized TV-NL4-3-CRF-gRNA constructs were replication-competent and highly stable during cell-culture passaging (Extended Data Fig. 1c). Thus, we introduced the 1537 different sgRNAs into the optimized backbone using homologous recombination. The proviral TV libraries yielded high levels of infectious virus after transfection into HEK293T cells (Extended Data Fig. 1d) and the mutations in the *nef* coding region did not compromise Nef expression (Extended Data Fig. 1e). Transformation of the proviral DNA library into *E. coli* resulted in ~3x10^5 colonies suggesting sufficient coverage to retain complexity. Deep sequencing confirmed that all 1537 sgRNAs were efficiently cloned into the backbone and that the genomic HIV-1 RNA sequences in the viral stocks reflected those in the proviral DNA TV library (Extended Data Fig. 1f). Altogether, our results showed that silent mutations in the TPI-region of *nef* together with intact *cis*-regulatory elements downstream of the U6-gRNA-scaffold cassette and upstream of the core enhancer in the 3`LTR allow efficient HIV-1 replication and stable sgRNA expression.

TVs reveal cellular factors restricting HIV-1 replication

To identify sgRNAs associated with a fitness advantage for HIV-1 replication, we infected CEM-M7-Cas9 cells with the pool of infectious TV-NL4-3-CRF-gRNA viruses targeting 511 potential antiviral genes. CXCR4-tropic HIV-1 NL4-3 IMCs replicate with fast kinetics. For passaging, we thus inoculated uninfected cells with 5% (v/v) of cell cultures obtained 2 days post-infection over a total period of 20 days (Fig. 1a). Virus containing culture supernatants were isolated in 5-day intervals. TV-NL4-3-CRF-gRNA viruses spread efficiently and

produced high levels of infectious virus (Extended Data Fig. 2a). Next generation sequencing (NGS) followed by bioinformatic analysis using MAGeCK[34] revealed the selection of TVs expressing sgRNAs targeting specific candidate antiviral genes in both the absence and presence of IFN-ß (Fig. 2a). Widening volcano plots illustrate that viruses containing sgRNAs conferring a replicative advantage are increasing over time (Fig. 2b). sgRNAs targeting some known restriction factors, such as IFITM1, TRIM5 and IFI16 were typically enriched by about 4- to 8-fold at the end of passage (Extended Data Fig. 2b). In comparison, TVs expressing sgRNAs targeting genes encoding Progranulin (PGRN), Class II MHC transactivator (CIITA), Coiled-Coil and C2 Domain Containing 1B (CC2D1B), Carcinoembryonic antigen-related cell adhesion molecule 3 (CEACAM3), Heme Oxygenase-1 (HMOX1) and Euchromatic Histone Lysine Methyl-transferase 2 (EHMT2, also named G9a) were increasingly enriched by up to several orders of magnitude (Fig. 2c, Extended Data Fig. 2c). The efficiency of selection varied between different sgRNAs targeting the same gene. However, the impact of individual sgRNAs on viral fitness was confirmed in the presence of IFN-β (Fig. 2c) and highly reproducible in independent experiments (Fig. 2d). TVs targeting *GRN*, *CIITA*, *CC2D1B*, *CEACAM3*, *HMOX1* and *EHMT2* also showed increased fitness in SupT1-CCR5-Cas9 cells (Figs. 2e, 2f, Extended Data Figs. 2c-e). Altogether, efficient and robust enrichment of the same specific sgRNAs in different experimental settings clearly indicated targeting of cellular genes suppressing HIV-1 replication.

GRN, CIITA and CEACAM3 restrict HIV-1 replication in primary CD4$^+$ T cells

To assess the significance of factors identified by the TV approach, we first confirmed that the protein products of genes targeted by gRNAs associated with increased fitness, i.e. GRN, CIITA, CC2D1B, CEACAM3, HMOX1 and EHMT2 are expressed in the cell lines used for selection (Fig. 3a). In agreement with our finding that TVs targeting these genes are selected in the presence and absence of IFN-β (Fig. 2), these six factors were expressed but (unlike ISG15 or tetherin) not further induced by IFN treatment (Fig. 3a). For functional analyses, we

initially focused on GRN as sgRNAs targeting the corresponding gene provided a substantial and robust fitness advantage (Fig. 2). *GRN* expresses an 88 kDa precursor, progranulin (PGRN) that has been reported to suppress HIV-1 transcription by interacting with cyclin T1[35,36]. In line with this, partial knock-out (KO) of PGRN in CEM-M7-Cas9 cells significantly increased infectious virus production (Fig. 3b). Overexpression of PGRN slightly reduced infectious virus production and protein expression of NL4-3 and (more clearly) the HIV-1 CH077 transmitted-founder IMC[9] in transfected HEK293T cells (Fig. 3c). Defects in viral accessory genes had little impact on the susceptibility of HIV-1 to PGRN (Fig. 3c). In support of an effect on viral transcription, PGRN inhibited LTR-driven luciferase expression in the absence and presence of Tat (Fig. 3d). In addition, PGRN reduced GFP expression by three proviral HIV-1 IRES-eGFP constructs in a dose-dependent manner (Fig. 3e). To further examine the significance of the antiviral activity of PGRN, we established a gRNA/Cas9-based KO approach for specific genes in primary $CD4^+$ T cells (Extended Data Fig. 3a). KO of PGRN reduced its protein levels by ~70% (Fig. 3f) and increased infectious virus production by WT HIV-1 NL4-3 and CH077 IMCs by ~2-fold (Fig. 3g, Extended Data 3b).

We next examined the effects of CIITA, CC2D1B and CEACAM3. Overexpression of these cellular factors had differential effects. CIITA had no significant impact on infectious virus yields (Fig. 4a) and increased LTR-driven eGFP production by proviral HIV-1 IRES-eGFP IMCs at very high expression levels (Extended Data Fig. 4a). In comparison, CC2D1B inhibited infectious virus production in a dose-dependent manner (Fig. 4a). Western blot analyses showed that CC2D1B significantly reduces virus release and Env processing (Extended Data Figs. 4b-d). This agrees with previous data showing that CC2D1A interferes with HIV-1 budding and that both CC2D1A and CC2D1B interact with the CHMP4 subunit of the ESCRT-III complex[37,38]. In contrast, high levels of CEACAM3 overexpression increased infectious virus production by transfected HEK293T cells (Fig. 4a).

To examine effects under more physiological conditions, we performed KO experiments in primary $CD4^+$ T cells. Protein expression was reduced by ~60% and ~80% for CIITA and CC2D1B, respectively, while no significant effect was observed for CEACAM3 (Extended Data Fig. 4e). Thus, it came as surprise that treatment with both CIITA and CEACAM3 targeting sgRNAs increased HIV-1 NL4-3 and CH077 replication in primary $CD4^+$ T cells by 2- to 3-fold, while KO of CC2D1B had no enhancing effect (Figs. 4b-d, Extended Data Fig. 4f). Notably, CEACAM3 is part of a large family of related adhesion molecules and antibody cross-reactivities may compromise meaningful analysis of specific KO efficiencies. To further examine the role of CC2D1B, we bypassed the early step of regular HIV-1 infection by utilizing *env*-defective single-round HIV-1 particles pseudo-typed with the VSV-G protein. In agreement with the inhibitory effect of CC2D1B overexpression on virus release (Extended Data Figs 4b, 4c), reduced CC2D1B expression moderated increased p24 antigen production under these experimental conditions (Fig. 4e). Altogether, our results showed that 3 of the 4 factors identified by the TV approach (PGRN, CIITA and CEACAM3) restrict HIV-1 replication in primary $CD4^+$ T cells. The remaining one (CC2D1B) reduced infectious virus release in overexpression assays and in primary $CD4^+$ T cells infected with VSV-G-pseudo-typed HIV-1 particles. This illustrates the power of TV-based screens in identifying relevant antiviral factors and further shows that some of them would be missed in commonly used overexpression and KO assays.

Increased fitness of CH077-based TVs targeting *HMOX1*, *EHMT2* and *RHOA*

Initially, we utilized NL4-3 because this HIV-1 IMC has been characterized and proven useful in numerous previous studies. However, NL4-3 is adapted for efficient replication in T cell lines. Thus, cellular factors restricting replication of primary patient-derived HIV-1 strains may be missed. To address this, we generated TV libraries of HIV-1 CH077 representing a TF HIV-1 IMC capable of using both CCR5 and CXCR4 for viral entry[9]. The initial constructs contain a duplication of the TPI and U3 regions in *nef* and the 3`LTR. To minimize recombination, we

codon optimized the *nef* gene with changes similar to the stabilizing changes in the NL4-3 proviral genome (Extended Data Figs. 1b, 5a). The optimized CH077 U6-gRNA-scaffold construct expressed functional Nef (Extended Data Fig. 5b). Viral infectivity was moderately reduced compared to the parental CH077 IMC (Extended Data Fig. 5c), presumably due to the slightly increased size of the viral genome. Nonetheless, the viral titers were well sufficient to cover all 1537 gRNAs and NGS confirmed that the virus stocks faithfully represented the proviral CH077-CRF-gRNA library (Extended Data Fig. 5d). TV-CH077-CRF-gRNA viruses spread efficiently but with slower kinetics than NL4-3 and produced high levels of infectious virus for ≥30 days of passaging (Extended Data Fig. 5e).

Replication of CH077-based TVs resulted in the selection of an overlapping but distinct set of sgRNAs compared to the NL4-3-based library (Figs. 5a, 5b). For example, the screen with the primary HIV-1 IMC confirmed that sgRNAs targeting *GRN*, *CC2D1B*, *CEACAM3*, *HMOX1* and *EHMT2* are associated with increased replication fitness (Fig. 5c). Notably, sgRNAs targeting *CEACAM3* were selected more efficiently by CH077-based compared to NL4-3-based TVs and sgRNAs targeting *RHOA* only increased fitness of CH077 but not NL4-3 (Figs. 5d, 5e). Ras homolog gene family member A (RhoA) is a small GTPase involved in actin cytoskeleton dynamics, cell motility and regulation of innate immunity[39]. Both enhancing and inhibitory effects on HIV-1 have been reported[40,41]. Overexpression of RhoA had no effect on HIV-1 NL4-3 but moderately affected infectious virus production by primary virus strains (Extended Data Fig. 6a). KO of RHOA was highly efficient but reduced, rather than enhanced, HIV-1 replication (Extended Data Figs. 6b, 6c). Further analyses showed that lack of RhoA increases cell death and impairs cell proliferation (Extended Data Figs. 6d-f), which explains why HIV-1 replication was reduced under these experimental conditions. Altogether, the TV-CH077-based screen confirmed the power of virus-driven identification of antiviral factors and suggests roles of CEACAM3 and RhoA in limiting primary HIV-1 replication.

***Nef*-defective TVs reveal novel potential Nef targets**

We hypothesized that lack of specific accessory genes will increase the selective advantage mediated by sgRNAs targeting restriction factors that are otherwise counteracted by these viral factors. To address this, we generated a TV-CRF-gRNA library using an otherwise isogenic *nef*-deleted HIV-1 NL4-3 as a backbone (Fig. 6a). We found that the Δ*nef*-TV-NL4-3-CRF-gRNA viruses replicated with moderately faster kinetics in CEM-M7-Cas9 cells compared to the parental constructs (Extended Data Fig. 7a), most likely because their genomic size is reduced by 360 bp. Altogether, results obtained using WT and Δ*nef* backbones correlated well and confirmed that sgRNAs targeting *GRN*, *HMOX1*, *CIITA* and *EHMT2* increase viral fitness (Fig. 6b, Extended Data Figs. 7b, 7c). Lack of Nef was associated with moderately increased selection efficiency of sgRNAs targeting IRF-3 (Extended Data Fig. 7c). IRF-3 is a major transcriptional regulator of type I IFN-dependent immune responses suggesting that they might be more effective against *nef*-deficient HIV-1. Predictably, lack of Nef promoted the selection of TVs expressing sgRNAs targeting genes encoding factors that are known to be counteracted by Nef, such as SERINC5[42,43] (Fig. 6c). The abundance of *SERINC5*-targeting sgRNAs increased with relatively slow kinetics, possibly because this factor affects virion infectivity and hence the inhibitory effect only becomes apparent over several rounds of replication.

Lack of an intact *nef* gene also increased the efficiency of selection for TV sgRNA variants targeting IFI16, especially in the presence of IFN-β (Figs. 6f-h). This came as surprise since we have previously shown that IFI16 inhibits most subtypes of HIV-1 by sequestering the transcription factors Sp1 and that clade C viruses evade this restriction by acquisition of an additional NF-kB binding site[44,45]. Analysis of five pairs of WT and *nef*-defective HIV-1 strains including two primary subtype B and two clade C IMCs confirmed that the latter are less sensitive to the inhibitory effects of IFI16 (Fig. 6i). In all cases, however, an intact *nef* gene clearly reduced viral susceptibility to IFI16 restriction (Fig. 6i). Thus, “handicapped” TVs lacking specific genes identify innate defense mechanisms that are counteracted by HIV-1 accessory proteins and reveal that inhibition by IFI16 is antagonized by Nef.

Discussion

In the present study, we exploited the replication fitness of infectious HIV-1 constructs expressing sgRNAs to decipher antiviral mechanisms. We named this technology "Traitor-virus" approach since populations of HIV-1 equipped with sgRNAs not only allow the pathogen to inactivate antiviral genes (i.e. confer a selective advantage) but also reveal their identity (i.e. the targeted sequence). Each sgRNA thus represents a unique molecular barcode allowing to associate a selection advantage with a specific cellular gene. Unlike previous methods, these virus-driven screens are highly effective, robust and sensitive because the effect of selective advantages associated with specific sgRNAs is amplified at each round of viral replication. Notably, this closely reflects the impact of fitness advantages during HIV-1 replication *in vivo*. Competition-based TV screens enable simultaneous evaluation of numerous cellular targets using complex HIV-1-U6-gRNA-scaffold libraries. Since the readout relies on changes in viral replication fitness and hence changes in the relative frequencies of sgRNAs our approach is highly robust and barely affected by variations in the number of input sgRNA copies. Functional analyses confirmed that TVs identify physiologically relevant cellular factors that restrict HIV-1 replication in primary $CD4^+$ T cells as well as a novel Nef targets.

We generated TVs expressing 1537 different gRNAs to assess 511 cellular target genes in two different viral backbones and in two Cas9 expressing cell lines. At the end of cell culture passage, sgRNAs targeting *GRN*, *CIITA*, *CC2D1B*, *CEACAM3*, *EHTM2* and *HMOX1* were enriched by ~10- to 500-fold under all selection conditions used demonstrating significant selection advantages for the virus. A clear advantage of TV-based screens is that they are highly flexible and allow to monitor differences in selective pressures in various cellular environments. Thus, they will allow to elucidate e.g. defense factors in T cells versus macrophages as well as innate immune mechanisms induced by different types of cytokines. Since inducibility by IFNs is a feature of many restriction factors, we performed the TV screen in the presence and absence of IFN-β. Unexpectedly, most antiviral factors identified were

expressed at similar levels and exerted comparable selection pressures under both conditions (Examples shown in Fig. 2). Notably, this was not due to lack of responsiveness of the Cas9 expressing CEM-M7 and SupT1-CCR5 cells since expression of ISG-15 and tetherin (BST-2) were efficiently induced by IFN-β treatment (Fig. 3a). Thus, our screen identifies antiviral factors that are induced by IFNs as well as those that are constitutively expressed to confer immediate protection. The latter may represent the real first line of defense as they do not require viral replication and innate immune activation to exert protective effects.

The high sensitivity and experimental setting of the virus-driven approach allows to identify factors that will be missed by current overexpression and KO studies. Overexpression confirmed inhibitory effects of PGRN and CC2D1B, while KO of GRN, CIITA and CEACAM3 increased HIV-1 replication in primary $CD4^+$ T cells. It is well known that overexpression in HEK293T cells is prone to artifacts and manipulation of viral target cells prior to infection, such as in KO settings, may yield misleading results. For example, the CD4 receptor is essential for HIV-1 entry but impairs viral release and infectivity later during the replication cycle[46]. Indeed, our results indicate that CC2D1B may promote viral entry but restrict replication/exit. In addition, KO of some cellular factors (such as RhoA) affects cell proliferation and viability precluding meaningful analysis. In the TV approach, HIV-1 itself drives selection and the fitness advantage is determined by the inhibitory effect of the targeted cellular gene. Thus, changes in the abundance of specific sgRNAs in the replicating viral population are a robust indicator of the importance of the corresponding antiviral factors.

Many previous screens focused on early steps of the HIV-1 replication cycle[22] and/or analyses of IFN-stimulated genes[23] mainly due to experimental constrains. In comparison, the TV-mediated inactivation of cellular genes is initiated after proviral integration simultaneously with viral gene expression. Thus, it detects cellular factors presumably affecting viral transcription and latency (IFI16, GRN, CIITA, EHMT2), assembly and release (tetherin, CC2D1B), as well as on virion infectivity (SERINC5, GBP5) (Extended data Fig. 8). Notably,

EHMT2 is a methyltransferase that generates H3K9me2, which plays an important role in HIV-1 latency in primary $CD4^+$ T cells[47]. Our results further support that silencing of EHTM2 promotes productive infection and efficient viral transcription. Thus, TV-based screens allow to identify targets for reactivation of latent viral reservoirs representing the major obstacle against a cure of HIV/AIDS[48]. HMOX1 is upregulated in response to oxidative stress and an important anti-inflammatory enzyme. It has been suggested to exert protective effects in HIV-1 infected individuals[49,50] and to restrict SARS-CoV-2[51,52]. We also observed enrichment of sgRNAs targeting IRF3, a transcription factor playing a key role in the induction of innate antiviral defense mechanisms indicating detection of factors setting the cell in an antiviral state rather than inhibiting HIV-1 directly.

In some aspects, the present TV method resembles a recently reported influenza-driven screen for virus dependency factors, which confirmed the attenuating role of TREX1 in viral sensing[53]. While having some similar perks as our system, such as allowing multiple rounds of replication that permit effective detection of fitness advantages, it relied on artificial induction of factors to identify proviral genes. A loss-of-function approach as in our case has the advantage of identifying cellular factors that affect viral replication at endogenous expression levels. Furthermore, compared to influenza virus, passaging of HIV-1 induces less cytopathic effects and thus loss of cells with increased replication. Most importantly, working with recombinant HIV-1 is established in a plethora of labs worldwide and screening systems based on lentiviruses are highly relevant as commonly usable, flexible and rapidly adoptable tools. In contrast, generation of genetically modified viruses containing segmented negative sense RNA genomes, such as influenza virus, requires technically challenging complex reverse genetics systems[54].

The ease of genetic manipulation of HIV-1-based constructs also allows generation of TVs with specific “handicaps”, such as defects in accessory genes, switches in coreceptor tropism or alterations in regulatory elements. For proof of concept, we generated and screened *nef*-

deleted NL4-3-based TVs. Predictably, lack of Nef increased the fitness advantage mediated by sgRNAs against *SERINC5*, an established Nef target[42,43]. Surprisingly, lack of Nef function also increased selection pressure for sgRNAs targeting *IFI16*. Overexpression analyses confirmed that *nef*-defective primary HIV-1 IMCs are significantly more susceptible to inhibition by IFI16 compared to otherwise isogenic WT viruses (Fig. 6i). IFI16 has been reported to inhibit viral pathogens including HIV-1 by a variety of mechanisms and has also been reported to play roles in innate sensing of viral pathogens[55–57]. Our finding that the inhibitory activity of IFI16 is not only evaded by an additional NF-κB binding site in the LTR of currently dominating clade C viruses[44] but also counteracted by Nef further supports an important role of this antiviral factors. Our results obtained using otherwise isogenic TV constructs differing in *nef* are proof-of-concept that genetically closely related pairs HIV-1 strains differing in IFN sensitivity and/or accessory gene function will pinpoint factors involved in virus transmission and/or counteracted by Vif, Vpr, Vpu or Nef. In addition, CRISPR/Cas9-based approaches become increasingly versatile. For example, mutated Cas9 allows to enhance gene expression for identification of HIV-1 dependency factors, or Cas12a2 allows targeting of mRNAs instead of KO in the genome[58].

Considering the nature of innate immune defenses, most, if not all factors identified in TV approach will be relevant for other viruses and diseases that involve innate immune responses, as well[2,59]. In fact, characterization of RFs against HIV-1 previously often served as a blueprint to identify important components of cellular defenses, such as APOBEC3, tetherin and SERINC proteins that are now well-known as broad anti-viral factors. Our TV approach identified HMOX1, which was previously shown to antagonize SARS-CoV-2[52]. CIITA provide cell resistance against Ebola virus and SARS-like coronaviruses[60]. Antiretroviral factors including APOBEC3 and TRIM proteins as well as SAMHD1 also play roles in genomic integrity and cancers[61,62]. Granulin (GRN) is known to be a potent mitogen implicated

in many human cancers[63]. These examples already demonstrate that factors identified in TV-approaches are of broad relevance.

In conclusion, we conceived an innovative pathogen-driven screening approach that provides an effective and convenient means to elucidate which cellular genes affect replication fitness of HIV-1. It is highly versatile and robust and thus will allow to assess zoonotic potential, degree of adaptation to human and/or the repertoire of their accessory genes to obtain exciting novel insights into the complex virus-host pathogens and defense mechanisms against viral pandemics. We present a focused screen but high cloning efficiencies and infectious virus titers offer the possibility for genome-wider unbiased identification of antiviral factors and comprehensive elucidation of complex virus-host interactions.

Acknowledgements

We thank Dré van der Merwe, Johannes Lang, Regina Burger, Jana-Romana Fischer, Birgit Ott, Daniela, Krnavek and Martha Meyer for technical assistance and Christina Stürzel for help with the generation of proviral constructs. Caterina Prelli Bozzo, Alexandre Laliberté and Chiara Pastorio are part of the International Graduate school for Molecular Medicine (IGradU). This study was supported by an ERC Advanced grant (Traitor-Viruses) to F.K. and DFG grants to F.K. (CRC 1279), K.M.J.S. (CRC 1279, SPP 1923, SP 1600/6-1) and a BMBF junior group to K.M.J.S. (IMMUNOMOD).

Author contributions

C.P.B. and A.L. performed most experiments with support by A.D.L., C.P. and M.V.. F.K. and K.M.J.S. conceived the study and planned experiments. S.K, A.G. and H.B. performed the deep-sequencing analyses. F.K. wrote the initial draft of the manuscript. All authors reviewed and approved the manuscript.

Declaration of Interests

All authors declare no competing interests.

Data and code availability

Further information and requests for resources and reagents should be directed to and will be fulfilled by FK (Frank.Kirchhoff@uni-ulm.de). All raw sequencing data files have been deposited in NCBI's Gene Expression Omnibus. All other data are available in the main text or the supplemental information.

Methods

Cell culture. All cells were cultured at 37°C in a 5% CO_2 atmosphere. Human embryonic kidney 293T cells (HEK293T; ATCC) and TZM-bl cells were maintained in Dulbecco's Modified Eagle Medium (DMEM) supplemented with 10% heat-inactivated fetal calf serum (FCS), L-glutamine (2 mM), streptomycin (100 µg/ml) and penicillin (100 U/ml). TZM-bl cells were provided and authenticated by the NIH AIDS Reagent Program, Division of AIDS, NIAID, NIH from Dr. John C. Kappes, Dr. Xiaoyun Wu and Tranzyme Inc. TZM-bl are derived from HeLa cells, which were isolated from a 30-year-old female. CEM-M7-Cas9 and SupT1 CCR5 high Cas9 cells were cultured in Roswell Park Memorial Institute (RPMI) 1640 Medium supplemented with 10% heat-inactivated fetal calf serum (FCS), L-glutamine (2 mM), streptomycin (100 µg/ml) and penicillin (100 U/ml).

Primary cell cultures. PBMCs from healthy human donors were isolated using lymphocyte separation medium (Biocoll separating solution; Biochrom) or lymphoprep (Stemcell). $CD4^+$ T cells were negatively isolated using the RosetteSep™ Human $CD4^+$ T Cell Enrichment Cocktail (Stem Cell Technologies # 15061) or the EasySep™ Human Naïve $CD4^+$ T cell Isolation Kit (Stem Cell Technologies #17953) according to the manufacturer's instructions. Primary cells were cultured in RPMI-1640 medium containing 10% FCS, glutamine (2 mM), streptomycin (100 µg/ml), penicillin (100 U/ml) and interleukin 2 (IL-2, Miltenyi Biotec #130-097-745) (10 ng/ml). The use of human PBMCs was approved by the Ethics Committee of the Ulm University Medical Center. All donors were anonymized and provided informed written consent.

Expression constructs. Expression vectors for GRN, CIITA, CC2D1B, RhoA, CEACAM3 were purchased from GenScript (#OHu25975C, #OHu21123C, #OHu11655C, # OHu26883C, # OHu15558C). Expression vector for IFI16 was previous described [45]. Constructs expressing the HIV-1 NL4-3 LTR and HIV-1 proviral constructs co-expressing eGFP via an IRES were generated as previously described[45].

Generation of cell lines constitutively expressing Cas9. To generate lentiviral backbones constitutively expressing Cas9, the ORF of Cas9 (humanized S. pyogenes Cas9 sequence) was fused to a nuclear localization signal and cloned behind a CMV promoter flanked by 3'LTR and 5'LTR sequences derived from HIV-1. Third generation lentiviral particles were produced by complementing the backbone in HEK293T cells with VSV-G, HIV-1 Gag/Pol and HIV-1 Rev expression vectors. $CD4^+$ T-cell lines (CEM-M7 and SupT1 CCR5 high) were transduced with the lentiviruses using spinoculation. 72h post transduction the cells were selected using 10µg/ml of Blasticidin. After the cells recovered for one-week, single cells were sorted in 96 well plates. Three weeks post sorting, single clone colonies were harvested and screened for Cas9 expression via Western blot analysis.

Construction of sgRNA library based on full length HIV-1. To generate the HIV-1 backbones, the gRNA cassette carrying the human U6 promoter and the invariant scaffold sgRNA sequence was inserted into the HIV-1 NL4-3 and HIV-1 CH077 pro-viral DNA between separated Nef and 3´LTR region using homologous recombination (NEB builder Hifi DNA assembly mastermix, NEB #E2621). The U6 promotor and the invariant scaffold are separated by a unique BsmBI restriction site using Q5® Site-Directed Mutagenesis Kit (NEB #E0554). Additional BsmBI restriction sites in the HIV-1 sequence were removed using Splicing by overhang extension (SOE) PCR (Forward Primer (Q5_del_BsmBI_CH077_F): 5'-AGCTCCCGGAcACGGTCACAG-3', Reverse Primer (Q5_del_BsmBI_CH077_R): 5'-GCATGTGTCAGAGGTTTTCAC-3', Forward Primer (Q5_del_BsmBI_NL4.3vec_F):

5'-CTGTGACCGTgTCCGGGAGCT-3', Reverse Primer (Q5_del_BsmBI_NL4.3vec_R): 5'-CTTGTCTGTAAGCGGATGCC-3', Forward Primer (Q5_del_BsmBI_NL4.3nef_F): 5'-AAAGAATGAGgCGAGCTGAGC-3', Reverse Primer (Q5_del_BsmBI_NL4.3nef_R): 5'-AAAGAATGAGgCGAGCTGAGC-3'. The nucleotide sequence of Nef was codon optimized to avoid recombination with the 3´ LTR: The fragment was synthetized by Twist Bioscience and cloned into the corresponding proviral DNA using XhoI/MluI (NL4-3) and KflI/MluI (CH077). For the generation of a small targeted library (BST2, GBP5, NT) oligonucleotides were purchased from Biomeres and designed with flanking regions in 3´(3'-GTGGAAAGGACGAAACACCG-5') and 5´ (3'-GTTTTAGAGCTAGAAATAG-3') of the gRNA overlapping with the backbone sequence to facilitate insertion by homologous recombination ((gRNA-GBP5-1): 5'-ACAATCGCTACCACAACTAC-3', (gRNA-GBP5-2): 5'-ATTAGTTCTGCTTGACACCG-3', (gRNA-BST2-1): 5'- CTGGATGCAGAGAAGGC-CCA-3', (gRNA-BST2-2): 5'- CTCTTCTTAGATGGCCCTAA-3', (gRNA-NT): 5'-ACGG-AGGCTAAGCGTCGCAA-3'). For the generation of the library targeting 511 genes, a pool of amplicons containing individual sgRNAs was purchased from Twist Bioscience. The variable sgRNA targeting sequences (18 nucleotides) were taken from the Gecko v2 library (3 for each gene). We selected gRNAs targeting 511 cellular genes sharing features of know restriction factors or proposed to play roles in HIV-1 infection[24,32]. To insert the sgRNA targeting sequences, the proviral backbones were linearized by using BsmBI. Recombination was performed by incubating the linearized vector (330 ng) with the amplicons pool (50 ng) and the NEBuilder HiFi DNA Assembly (NEB #E2621) 50°C for 15 minutes to one hour. Afterwards, the reaction was purified using the Monarch DNA Gel Extraction Kit (NEB #T1020L) and transformed by electroporation using the Gene Pulser Xcell (1700 V, 25 µF, 200 Ω, 1 pulse, Biorad) in C2989 5alpha electrocompetent bacteria (NEB, #C3020K). After the bacteria recovered for one hour at 37°C in SOC medium, they were plated on 6 15cm agarose dishes and incubated at 30°C for 40 hours. All colonies were collected by scraping and

the DNA was extracted using the Plasmid maxiprep (Qiagen #12165). For a small proof-of-principle library containing 7 different targets, sgRNA integration and complexity of the library was quantified using SYBR-green qPCR (SYBR™ Green PCR Master Mix, Applied Biosystems #4309155) with one forward primer binding the U6 promoter region and specific reverse primers for each sgRNA. To generate NL4-3 TVs mutants lacking the Nef gene, we introduced a stop codon at the beginning *nef* and subsequentially we deleted 360 nucleotides (from nucleotide 261 to 621, Stop Codon NL4-3 Nef Forward: 5´-CTATAAGATG-TAGTAAAAGTGGTCAAAAAGTAGTG-3´, Stop Codon NL4-3 Nef Reverse: 5´-CAAAA-TCCTTTCCAAGCC-3´, Nef deletion Forward: 5´-ACGCGTCCAAGGTCGGGC-3´, Nef deletion Reverse: 5´-AGATCTACAGCTGCCTTGTAAGTCATTGG-3´) using Q5® Site-Directed Mutagenesis Kit (NEB #E0554S).

Verification of viral recombination by PCR. To check for recombination and loss of the cassette during passaging, viral RNA was isolated at different time points with the QIAamp Viral RNA Mini Kit (Qiagen # 52906). cDNA was synthetized using the PrimeScript™ RT Reagent Kit (Takara #RR037A) according to the manufacturer's instructions. The cassette was amplified using flanking primers (Forward Primer (PCR_Recombination_F): 5'-GTGGA-ACTTCTGGGA-3', Reverse Primer (PCR_Recombination_R): 5'-ACTGCTAGAGATTTT-CCACACTGACTAAAAG-3'. PCR reactions were loaded onto a 1% agarose and ran at 140V for 30 min.

Stimulation with type I and II interferons. One million CEM-M7 or SupT1 CC5 cells were seeded in 1mL RPMIXXX in 12-well plates. Cells were stimulated with IFN-α (500 U/ml, R&D systems 11100-1), IFN-β (500 U/ml, R&D systems 8499-IF-010) or IFN-γ (200 U/ml, R&D systems 285-IF-100). 24 hours post-stimulation whole cell lysates were generated.

CRISPR/Cas9 KO in T cells. $CD4^+$ T lymphocytes were isolated from healthy donors as described above. Cells were stimulated with IL-2 (10 ng/ml) (Miltenyi Biotec #130-097-745)

and with anti-CD3/CD28 beads (Gibco #11132D) for 3 days. Cells were cultured in RPMI-1640 medium containing 10% FCS and IL-2 (10 ng/ml). 1×10^6 primary CD4+T cells (stimulated) or 1×10^6 CEM-M7 Cas9 cells were transfected with the HiFi Cas9 Nuclease V3 (IDT)/gRNA complex (80 pmol/300 pmol) (Lonza) using a non-targeting or a GRN(5´-GCGATCCTGCTTCCAAAGATC-3´), CIITA (5´-GCCCCTAGAAGGTGGCTACC-3´), RHOA (5´-TATCGAGGTGGATGGAAAGC-3´), CC2D1B (5´-GAGTTGGCGGCAGA-CTGTATG-3´), CEACAM3(5´-GTGTCTCTCGACCGCTGTTTG-3´)-specific sgRNAs or NT control (5´-ACGGAGGCTAAGCGTCGCAA-3´), using the Amaxa 4D-Nucleofector Human Activated T Cell P3 Lonza Kit (Lonza #V4XP-3032), pulse code EO115. At four- and three- days post Cas9/sgRNA-transfection respectively, 1 million cells/sample were infected with the indicated HIV-1 strains by spinoculation. From 2 to 5 or 6 dpi, supernatants were harvested and infectious virus yield via the TZM-bl reporter cells assay.

Transfection and production of viral stocks. HEK293T cells were transiently transfected using TransIT-LT1 (Mirus #MIR2306) according to the manufacturer's protocol at a ratio of 3µL of transfection reagent per 1µg of DNA and the medium was replaced 24 hours post transfection. To test the antiviral effect of potential restriction factors, pcDNA-based expression constructs cotransfected with the proviral constructs. Whenever different amounts of pcDNA expression vectors were used within an experiment, empty vector control plasmids were used to keep the total DNA amount constant for all samples. The transfected cells were incubated for 8-16 h before the medium was replaced by fresh supplemented DMEM. To generate virus stocks, one day before transfection, 10 mio cells were seeded in 15 cm dishes in 20 ml medium to obtain a confluence of 70-80% at the time of transfection. For transfection, 25µg of DNA was mixed with 75µl LT1, incubated 20 min at RT and added dropwise to the cells. 48 hours post transfection, the virus was harvested, centrifuged 5 min at 2000rpm and concentrated 10 times using Amicon® Ultra 15 mL Filters (Merck #UFC910096). The concentrated virus aliquoted and stored at -80°C.

VSV-G-pseudo-typed HIV-1. To generate VSV-G-pseudo-typed HIV-1, HEK293T cells were transiently transfected using the calcium-phosphate precipitation method as previously described[45]. Briefly 5µg of proviral DNA and 1µg of expression plasmids for VSV-G was mixed with 13 µl 2 M CaCl2 and filled up with water to 100 µl Afterwards, 100 µl of 2 x HBS was added dropwise to this mixture, which was mixed by pipetting and added dropwise to the cells seeded in 6 well plates.

Infection, kinetic and traitor virus enrichment. To start the replication kinetic, 1 million cells were infected with the indicated HIV-1 library constructs via spinoculation (2h at 26°C). Afterwards cells were washed three times with RPMIxxx and seeded in 6 well plates at a cell density of 1 million/ml. Every two to three days, infection was monitored by flow cytometry (see below). When infection was higher than 20%, it was reduced to 1% for the next 2 days by addition of uninfected cells. From 5dpi, cells were treated with IFN-β (R&D Systems #8499-IF-010, 1000U/ml for CEM-M7 Cas9 and 100U/ml for SupT1 CCR5 high Cas9) and IFN-β was refreshed every three days.

Viral RNA preparation for sequencing. Viral RNA levels were determined in supernatants collected from HIV-1 infected cells at 5, 10, 15, 20, 30- and 40-days post-infection. Total RNA was isolated using the Viral RNA Mini Kit (Qiagen) according to the manufacturer's instructions. cDNA reactions were performed according to the manufacturer's instructions of the PrimeScript™ RT Reagent Kit (Takara) using primers specifically targeting the U6 and scaffold region (forward primer 5´-CCGACTCGGTGCCACTTTTT-3´, reverse primer 5´-CGTGACGTAGAAAGTAATAATTT-CTTGGG-3´). cDNA reactions were purified using the Monarch PCR Purification Kit (NEB #T1030L) and eluted in 10µl elution buffer. The gRNA cassette was amplified using the NEBNext® High-Fidelity 2X PCR Master Mix (NEB) and primers including Illumina adaptors and 8nt barcodes to allow Next Generation

Sequencing analysis (Supplementary Table 2). PCR reactions were purified using the Monarch PCR Purification Kit (NEB # T1030L) and eluted in 10µl elution buffer.

Next Generation sequencing. NGS was performed using the Illumina NextSeq2000 platform with 60 base-pair paired-end runs. Raw reads were demultiplexed, trimmed, groomed according to quality and aligned to the custom library sequences using the MAGeCK algorithm suite on the Galaxy platform. Individual read counts are determined and median-normalized to for the effect of library sizes and read count distributions. Individual sgRNAs targeting the same gene are summarized, and a variance model calculated using a negative binomial model to statistically assess the difference between control (input) and the conditions (different days). Targets are ranked by MAGeCK according to their *p*-value via a modified robust ranking aggregation (RRA) algorithm (α-RRA) to identify enriched genes. Overrepresented sgRNA sequences compared to the input control represent viruses that had a sgRNA targeting a gene, that restricts viral replication. Volcano plots were generated using R version 4.1.1 and ggplot2 version 3.3.5.

Venn diagrams. List of enriched genes were generated for each condition by selecting genes based on the positive MAGeCK score. Genes were considered enriched when the $-\log_{10}$ of the positive score was above 1.5. Genes overlap of the lists was calculated using the bioinformatics tool from UGent .https://bioinformatics.psb.ugent.be/webtools/Venn/.

SYBR Green qPCR. To determine the relative enrichment of GBP5 and BST2 gRNAs over time compared to the NT, we performed RT-qPCR using the SYBR Green PCR Master Mix (Applied Biosystems #A25742) following the manufacturer protocol. In brief, we diluted the cDNA and we perform the RT-qPCR reactions using specific primers flanking the gRNAs regions (U6 Forward_SYBR: 5´-AGAATTAATTTGACTGTAAACACAAAGATATTAG-3´, GBP5-1gRNA Reverse_SYBR: 5´-CGTAGTTGTGGTAGCGATTGT-3´, GBP5-2 gRNA Reverse_SYBR: 5´-CGGTGTCAAGCAGAACTAAT-3´, BST2-1 gRNA Reverse_SYBR: 5´-

GGCCTTCTCTGCATCCAG-3´, BST2-2 gRNA Reverse_SYBR: 5´-AACTTAGGGC-CATCTAAGAAGAG-3´, NT gRNA Reverse_SYBR: 5´-TTGCGACGCTTAGCCTC-3´). Values were normalized on the values from 3dpi.

Supernatants and whole cell lysates. To determine expression of cellular and viral proteins, cells were washed in PBS and subsequently lysed in Western blot lysis buffer (150 mM NaCl, 50 mM HEPES, 5mM EDTA, 0.1% NP40, 500 µM Na_3VO_4, 500 µM NaF, pH 7.5) or radioimmunoprecipitation assay (RIPA) buffer (50 mM Tris-HCl; pH 7.4, 150 mM NaCl, 1% (v/v) NP-40, 0.5% (w/v) deoxycholic acid (DOC), 0.1% (w/v) SDS) supplemented with protease inhibitor (Roche, 1:500). After 5 min of incubation on ice, samples were centrifuged (4°C, 20 min, 14.000 rpm) to remove cell debris. The supernatant was transferred to a fresh tube, the protein concentration was measured with Pierce™ Rapid Gold BCA Protein Assay Kit (Thermofisher) and adjusted using Western blot lysis buffer. Supernatants were centrifuged on top of a 20% sucrose layer in at 21,000 g for 2 hours. The viral pellet was then lysed in Western blot lysis buffer with 4x Protein Sample Loading Buffer (LICOR) supplemented with 10% β-mercaptoethanol (Sigma Aldrich) and heated at 95°C for 5 min.

SDS-PAGE and Immunoblotting. Western blotting was performed as previously described[64]. In brief, whole cell lysates were mixed with 4x Protein Sample Loading Buffer (LI-COR, at a final dilution of 1x) supplemented with 10% β-mercaptoethanol (Sigma Aldrich), heated at 95°C for 5 min, separated on NuPAGE 4±12% Bis-Tris Gels (Invitrogen) for 90 minutes at 100 V and blotted onto Immobilon-FL PVDF membranes (Merck Millipore). The transfer was performed a constant voltage of 30 V for 30 minutes using semi-dry transfer system. For larger proteins (Cas9, EHMT2), transfer was performed at a constant Amperage 0,4 A for 2 hours using a wet transfer system. After the transfer, the membrane was blocked in 1 % Casein in PBS (Thermo Scientific). Proteins were stained using primary antibodies against PGRN (Abcam #ab208777, 1 :200), CIITA (Santa Cruz #sc-13556, 1:200), EHMT2 (Cell Signalling

#3306, 1:200), CC2D1B (Proteintech #20774-1-AP , 1:500), HMOX1 (Sigma MA1-112, 1:200), BST2 (Proteintech 13560-1-AP, 1:500), GBP5 (Santa Cruz #sc-1603539, 1:200), CEACAM3 (Abcam #ab196606, 1:200), ISG15 (Santa Cruz #sc-166755, 1:200), IFI16 (Santa Cruz #sc-8023, 1:150), RHOA (Abcam #ab54835, 1:200), GAPDH (Biolegend #607902, 1:1000), Cas9 (Cell Signalling #14697, 1:1000), HIV-1 p24 (Abcam #6604667, 1:1000) HIV-1 Env (NIH AIDS Reagents program #ARP-12559, 1:1000), HIV-1 Nef (NIH AIDS Reagents program #ARP-1539, 1:500) and Infrared Dye labelled secondary antibodies (IRDye® 680RD Goat anti-Rabbit IgG (H + L), LI-COR #926-68071, 1:10,000; IRDye® 800CW Goat anti-Mouse IgG (H + L), LI-COR #926-32210, 1:10,000; IRDye® 800CW Goat anti-Rabbit IgG (H + L), LI-COR #926-32211, 1:10,000; IRDye 800RD Goat anti-Rat IgG (H + L), LI-COR #925-32219, 1:10,000; IRDye 680RD Goat anti-Rat IgG (H + L), LI-COR #926-68071, 1:10,000). Band intensities were quantified using Image Studio (LI-COR).

Flow Cytometry. To monitor infection during the replication kinetic, flow cytometry was used to quantify the infected cells. For CEM-M7 Cas9 kinetics, ~400,000 cells were harvested, washed once with PBS and stained for 15min at RT in the dark with eBioscience Fixable viability dye 780 (ThermoFisher Scientific, 1:1000 in PBS). Cells were washed twice with PBS and fixed in 2% PFA for 30 min at 4°C. For SupT1 CCR5 high Cas9 kinetic and to monitor KO efficiencies in cells infected with HIV-1 either carrying the NT or BST2 or GBP5 gRNA, ~400,000 cells were harvested, washed once with PBS and stained for 30 min at RT in the dark with anti-CD4 antibody (PerCP-Cy5.5, Biolegend #317428, 1:50 in PBS) and eBioscience Fixable viability dye 780 (ThermoFisher Scientific #65-0865-14, 1:1000 in PBS). Afterwards cells were washed twice with PBS and permeabilized 20 minutes with 200µl BD Cytofix/Cytoperm™ Fixation/Permeabilization Solution Kit (BD Biosciences)at RT. Cells were washed twice with 200µl BD 1X Perm/Wash solution and stained 1h at 4°C with anti-HIV-1 p24 (RD1/PE, Beckman Coulter #6604667, 1:100 in 1X BD Perm/wash solution) or anti-BST2 (Proteintech #13560-1-AP, 1:100 in 1X Perm/Wash solution) or anti-GBP5 (Santa

Cruz #sc-1603539, 1:100 in 1X Perm/Wash solution). After washing twice with 1X Perm/Wash solution, wells were either stained with secondary antibody goat anti rabbit (PE, Abcam ab97070, 1:100 in 1X Perm/Wash) or fixed in 2% PFA for 30 min at 4°C. After 1 hours at 4°C, cells stained with secondary antibodies were washed twice with 200µL 1X BD Perm/Wash solution and fixed with 2% PFA for 30 min at 4°C. Cells were acquired with BD FACSCanto II Flow Cytometer (BD Biosciences).

Effects of GRN and CIITA on LTR-driven eGFP expression. HEK293T cells were co-transfected with expression constructs for GRN or CIITA and HIV-1 NL4-3, CH077 and CH058 proviral constructs co-expressing eGFP via an IRES. 48 hours after transfection cells were harvested, washed in 500µl PBS and stained for 15min at RT in the dark with eBioscience Fixable viability dye 780 (ThermoFisher Scientific #65-0865-14, 1:1000 in PBS). Afterwards cells were permeabilized 20 minutes with 200µl BD Cytofix/Cytoperm™ Fixation/Permeabilization Solution Kit (BD Biosciences)at RT, afterwards washed twice with 200µl BD 1X Perm/Wash solution. Cells were stained with anti-GRN (Abcam #ab208777, 1 100 in 1X BD Perm/Wash solution) or anti-CIITA (AF647, Santa Cruz #sc-13556, 1:100 in 1X BD Perm/Wash solution) for 1h at 4°C. After washing twice with 200µl BD 1X Perm/Wash cells stained with conjugated CIITA antibody were fiyed in 2% PFA for 30 min at 4°C.Cells stained with GRN antibody were stained 1 hour at 4°C with secondary antibody goat anti rabbit (PE, Abcam #ab97070, 1:100 in 1X Perm/Wash). Cells were washed twice with 200µL BD 1XPerm/Wash solution and fixed in 2% PFA for 30 min at 4°C. Cells were acquired on BD FACSCanto II Flow Cytometer (BD Biosciences). Mean fluorescence intensities (MFI) of eGFP in the GRN+/eGFP+ or CIITA+/eGFP+ population was determined.

Viral promoter activity. To determine the effect of GRN on the activity of different viral promoters, 135,000 HEK293T cells/well were seeded in 24 well plates. Cells were cotransfected with firefly luciferase reporter constructs (5 ng) under the control of the HIV-1

LTR or the CMV IE promoter and expression constructs for GRN (50 ng) or a vector control using the calcium phosphate method. In some cases, expression constructs for HIV-1 NL4-3 Tat (500 pg) were cotransfected to activate the LTR promoter. 40 h post-transfection, cells were lysed and firefly luciferase activity was determined.

Luciferase assay. To determine LTR expression, the cells were lysed in 300µl of Luciferase Lysis buffer (Promega #E1531) and firefly luciferase activity was determined using the Luciferase Assay Kit (Promega #E1501) according to the manufacturer's instructions on an Orion microplate luminometer (Berthold).

Viral infectivity. To determine infectious virus yield, 10,000 TZM-bl reporter cells/well were seeded in 96-well plates and infected with cell culture supernatants in triplicates on the following day. Three days post-infection, cells were lysed and *β-galactosidase* reporter gene expression was determined using the X-GalScreen Kit (Applied Bioscience #T1027) according to the manufacturer's instructions with an Orion microplate luminometer (Berthold).

ELISA p24 and virion infectivity analysis. HIV-1 p24 amounts in cell culture supernatants were determined using an in-house ELISA. Briefly, 96-well MaxiSorp microplates (Sigma) were coated with 0.5 mg/ml anti-HIV-1 p24 (EXBIO #11-CM006-BULK) and incubated in a wet chamber at RT overnight. The plates were then washed 3 times with PBS-T (PBS and 0.05% Tween 20) and incubated with blocking solution (PBS and 10% (v/v) FCS) for 2 hours at 37°C. After washing, the plates were loaded with 100 µL serial dilution of HIV-1 p24 protein (Abcam #ab43037) as standard and dilutions of virus supernatants lysed with 1% (v/v) Triton X-100 and incubated overnight in a wet chamber at RT. After washing unbound capsid, 100 µl/well polyclonal rabbit antiserum against p24 antigen (Eurogentec, 1:1,000 in PBS-T with 10% (v/v) FCS) was added for 1 hour at 37°C. After washing, 100 µL of goat anti-rabbit HRP-coupled antibody (Dianova #111-035-008, 1:2,000) was loaded on the plates and incubated for one hour at 37°C. Finally, the plates were washed and 100 µL SureBlue TMB 1-Component

716 Microwell Peroxidase Substrate (Medac #52-00-04) was added. After 20 minutes shaking at
717 450 rpm and RT, the reaction was stopped with 0.5 M H_2SO_4 (100 µl/well). The optic density
718 was determined by comparing with a standard curve and measured at 450 nm and 650 nm with
719 the Thermo Max microplate reader (Molecular devices).

720 **Statistics.** Statistical analyses were performed using GraphPad PRISM 10 (GraphPad
721 Software). P-values were determined using a two-tailed Student's t test with Welch's correction
722 or Two-way Anova with Sidak´s multiple comparison. Unless otherwise stated, data are shown
723 as the mean of at least three independent experiments ± SEM. Significant differences are
724 indicated as: *, $p < 0.05$; **, $p < 0.01$; ***, $p < 0.001$. Statistical parameters are specified in
725 the figure legends.
726

References

1. Bieniasz, P.D. (2004). Intrinsic immunity: a front-line defense against viral attack. Nature immunology *5*, 1109–1115. 10.1038/ni1125.

2. Kluge, S.F., Sauter, D., and Kirchhoff, F. (2015). SnapShot: antiviral restriction factors. Cell *163*, 774-774.e1. 10.1016/j.cell.2015.10.019.

3. Towers, G.J., and Noursadeghi, M. (2014). Interactions between HIV-1 and the cell-autonomous innate immune system. Cell Host and Microbe *16*, 10–18. 10.1016/j.chom.2014.06.009.

4. Harris, R.S., Hultquist, J.F., and Evans, D.T. (2012). The Restriction Factors of Human Immunodeficiency Virus. Journal of Biological Chemistry *287*, 40875–40883. 10.1074/jbc.R112.416925.

5. Malim, M.H., and Bieniasz, P.D. (2012). HIV Restriction Factors and Mechanisms of Evasion. Cold Spring Harbor Perspectives in Medicine *2*, a006940–a006940. 10.1101/cshperspect.a006940.

6. Sauter, D., and Kirchhoff, F. (2019). Key Viral Adaptations Preceding the AIDS Pandemic. Cell Host & Microbe *25*, 27–38. 10.1016/j.chom.2018.12.002.

7. Gupta, R.K., and Towers, G.J. (2009). A tail of Tetherin: how pandemic HIV-1 conquered the world. Cell Host Microbe *6*, 393–395. 10.1016/j.chom.2009.11.002.

8. Sharp, P.M., and Hahn, B.H. (2011). Origins of HIV and the AIDS pandemic. Cold Spring Harbor perspectives in medicine *1*, a006841. 10.1101/cshperspect.a006841.

9. Ochsenbauer, C., Edmonds, T.G., Ding, H., Keele, B.F., Decker, J., Salazar, M.G., Salazar-Gonzalez, J.F., Shattock, R., Haynes, B.F., Shaw, G.M., et al. (2012). Generation of Transmitted/Founder HIV-1 Infectious Molecular Clones and Characterization of Their Replication Capacity in CD4 T Lymphocytes and Monocyte-Derived Macrophages. Journal of Virology *86*, 2715–2728. 10.1128/jvi.06157-11.

10. Parrish, N.F., Gao, F., Li, H., Giorgi, E.E., Barbian, H.J., Parrish, E.H., Zajic, L., Iyer, S.S., Decker, J.M., Kumar, A., et al. (2013). Phenotypic properties of transmitted founder HIV-1. Proceedings of the National Academy of Sciences of the United States of America *110*, 6626–6633. 10.1073/pnas.1304288110.

11. Kmiec, D., Iyer, S.S., Stürzel, C.M., Sauter, D., Hahn, B.H., and Kirchhoff, F. (2016). Vpu-Mediated Counteraction of Tetherin Is a Major Determinant of HIV-1 Interferon Resistance. mBio *7*, e00934-16. 10.1128/mBio.00934-16.

12. Wu, Y., Olety, B., Weiss, E.R., Popova, E., Yamanaka, H., and Göttlinger, H. (2019). Potent enhancement of HIV-1 replication by nef in the absence of SERINC3 and SERINC5. mBio *10*. 10.1128/mBio.01071-19.

13. Bartok, E., and Hartmann, G. (2020). Immune Sensing Mechanisms that Discriminate Self from Altered Self and Foreign Nucleic Acids. Immunity *53*, 54–77. 10.1016/j.immuni.2020.06.014.

14. Braun, E., and Sauter, D. (2019). Furin-mediated protein processing in infectious diseases and cancer. Clinical & Translational Immunology *8*. 10.1002/cti2.1073.

15. Colomer-Lluch, M., Ruiz, A., Moris, A., and Prado, J.G. (2018). Restriction Factors: From Intrinsic Viral Restriction to Shaping Cellular Immunity Against HIV-1 (NLM (Medline)) 10.3389/fimmu.2018.02876.

16. Diamond, M.S., and Farzan, M. (2013). The broad-spectrum antiviral functions of IFIT and IFITM proteins (Nature Publishing Group) 10.1038/nri3344.

17. Dias Junior, A.G., Sampaio, N.G., and Rehwinkel, J. (2019). A Balancing Act: MDA5 in Antiviral Immunity and Autoinflammation (Elsevier Ltd) 10.1016/j.tim.2018.08.007.

18. Goodier, J.L., Pereira, G.C., Cheung, L.E., Rose, R.J., and Kazazian, H.H. (2015). The Broad-Spectrum Antiviral Protein ZAP Restricts Human Retrotransposition. PLoS genetics *11*, e1005252. 10.1371/journal.pgen.1005252.

19. Jouvenet, N., Neil, S.J.D., Zhadina, M., Zang, T., Kratovac, Z., Lee, Y., McNatt, M., Hatziioannou, T., and Bieniasz, P.D. (2009). Broad-Spectrum Inhibition of Retroviral and Filoviral Particle Release by Tetherin. Journal of Virology *83*, 1837–1844. 10.1128/jvi.02211-08.

20. Massa, D., Baran, M., Bengoechea, J.A., Bowie, A.G., and Voelker, D.R. (2020). PYHIN1 regulates pro-inflammatory cytokine induction rather than innate immune DNA sensing in airway epithelial cells. Journal of Biological Chemistry *295*, 4438–4450. 10.1074/jbc.RA119.011400.

21. Olson, M.E., Harris, R.S., and Harki, D.A. (2018). APOBEC Enzymes as Targets for Virus and Cancer Therapy. Cell Chem Biol *25*, 36–49. 10.1016/j.chembiol.2017.10.007.

787 22. Jones, C.E., Tan, W.S., Grey, F., and Hughes, D.J. (2021). Discovering antiviral restriction
788 factors and pathways using genetic screens. J Gen Virol *102*, 001603.
789 10.1099/jgv.0.001603.

790 23. Kane, M., Zang, T.M., Rihn, S.J., Zhang, F., Kueck, T., Alim, M., Schoggins, J., Rice,
791 C.M., Wilson, S.J., and Bieniasz, P.D. (2016). Identification of Interferon-Stimulated
792 Genes with Antiretroviral Activity. Cell Host & Microbe *20*, 392–405.
793 10.1016/j.chom.2016.08.005.

794 24. McLaren, P.J., Gawanbacht, A., Pyndiah, N., Krapp, C., Hotter, D., Kluge, S.F., Götz, N.,
795 Heilmann, J., Mack, K., Sauter, D., et al. (2015). Identification of potential HIV restriction
796 factors by combining evolutionary genomic signatures with functional analyses.
797 Retrovirology *12*, 41. 10.1186/s12977-015-0165-5.

798 25. Liu, S.-Y., Sanchez, D.J., and Cheng, G. (2011). New developments in the induction and
799 antiviral effectors of type I interferon. Current Opinion in Immunology *23*, 57–64.
800 10.1016/j.coi.2010.11.003.

801 26. OhAinle, M., Helms, L., Vermeire, J., Roesch, F., Humes, D., Basom, R., Delrow, J.J.,
802 Overbaugh, J., and Emerman, M. (2018). A virus-packageable CRISPR screen identifies
803 host factors mediating interferon inhibition of HIV. eLife *7*. 10.7554/eLife.39823.

804 27. Neil, S.J.D., Zang, T., and Bieniasz, P.D. (2008). Tetherin inhibits retrovirus release and is
805 antagonized by HIV-1 Vpu. Nature *451*, 425–430. 10.1038/nature06553.

806 28. Van Damme, N., Goff, D., Katsura, C., Jorgenson, R.L., Mitchell, R., Johnson, M.C.,
807 Stephens, E.B., and Guatelli, J. (2008). The Interferon-Induced Protein BST-2 Restricts
808 HIV-1 Release and Is Downregulated from the Cell Surface by the Viral Vpu Protein. Cell
809 Host & Microbe *3*, 245–252. 10.1016/j.chom.2008.03.001.

810 29. Braun, E., Hotter, D., Koepke, L., Zech, F., Groß, R., Sparrer, K.M.J., Müller, J.A., Pfaller,
811 C.K., Heusinger, E., Wombacher, R., et al. (2019). Guanylate-Binding Proteins 2 and 5
812 Exert Broad Antiviral Activity by Inhibiting Furin-Mediated Processing of Viral Envelope
813 Proteins. Cell Reports *27*, 2092-2104.e10. 10.1016/j.celrep.2019.04.063.

814 30. Krapp, C., Hotter, D., Gawanbacht, A., McLaren, P.J., Kluge, S.F., Stürzel, C.M., Mack,
815 K., Reith, E., Engelhart, S., Ciuffi, A., et al. (2016). Guanylate Binding Protein (GBP) 5 Is
816 an Interferon-Inducible Inhibitor of HIV-1 Infectivity. Cell Host & Microbe *19*, 504–514.
817 10.1016/j.chom.2016.02.019.

31. Hsu, M., Harouse, J.M., Gettie, A., Buckner, C., Blanchard, J., and Cheng-Mayer, C. (2003). Increased mucosal transmission but not enhanced pathogenicity of the CCR5-tropic, simian AIDS-inducing simian/human immunodeficiency virus SHIV(SF162P3) maps to envelope gp120. J Virol *77*, 989–998. 10.1128/jvi.77.2.989-998.2003.

32. Mahé, D., Matusali, G., Deleage, C., Alvarenga, R.L.L.S., Satie, A.-P., Pagliuzza, A., Mathieu, R., Lavoué, S., Jégou, B., de França, L.R., et al. (2020). Potential for Virus Endogenization in Humans through Testicular Germ Cell Infection: the Case of HIV. J Virol *94*, e01145-20. 10.1128/JVI.01145-20.

33. Shalem, O., Sanjana, N.E., Hartenian, E., Shi, X., Scott, D.A., Mikkelsen, T.S., Heckl, D., Ebert, B.L., Root, D.E., Doench, J.G., et al. (2014). Genome-Scale CRISPR-Cas9 Knockout Screening in Human Cells. Science *343*, 84–87. 10.1126/science.1247005.

34. Li, W., Xu, H., Xiao, T., Cong, L., Love, M.I., Zhang, F., Irizarry, R.A., Liu, J.S., Brown, M., and Liu, X.S. (2014). MAGeCK enables robust identification of essential genes from genome-scale CRISPR/Cas9 knockout screens. Genome Biol *15*, 554. 10.1186/s13059-014-0554-4.

35. Hoque, M., Tian, B., Mathews, M.B., and Pe'ery, T. (2005). Granulin and granulin repeats interact with the Tat.P-TEFb complex and inhibit Tat transactivation. J Biol Chem *280*, 13648–13657. 10.1074/jbc.M409575200.

36. Hoque, M., Young, T.M., Lee, C.-G., Serrero, G., Mathews, M.B., and Pe'ery, T. (2003). The growth factor granulin interacts with cyclin T1 and modulates P-TEFb-dependent transcription. Mol Cell Biol *23*, 1688–1702. 10.1128/MCB.23.5.1688-1702.2003.

37. Usami, Y., Popov, S., Weiss, E.R., Vriesema-Magnuson, C., Calistri, A., and Göttlinger, H.G. (2012). Regulation of CHMP4/ESCRT-III function in human immunodeficiency virus type 1 budding by CC2D1A. J Virol *86*, 3746–3756. 10.1128/JVI.06539-11.

38. Martinelli, N., Hartlieb, B., Usami, Y., Sabin, C., Dordor, A., Miguet, N., Avilov, S.V., Ribeiro, E.A., Göttlinger, H., and Weissenhorn, W. (2012). CC2D1A Is a Regulator of ESCRT-III CHMP4B. Journal of Molecular Biology *419*, 75–88. 10.1016/j.jmb.2012.02.044.

39. Bros, M., Haas, K., Moll, L., and Grabbe, S. (2019). RhoA as a Key Regulator of Innate and Adaptive Immunity. Cells *8*, 733. 10.3390/cells8070733.

40. Loomis, R.J., Holmes, D.A., Elms, A., Solski, P.A., Der, C.J., and Su, L. (2006). Citron Kinase, a RhoA Effector, Enhances HIV-1 Virion Production by Modulating Exocytosis. Traffic (Copenhagen, Denmark) *7*, 1643. 10.1111/j.1600-0854.2006.00503.x.

41. Lucera, M.B., Fleissner, Z., Tabler, C.O., Schlatzer, D.M., Troyer, Z., and Tilton, J.C. (2017). HIV signaling through CD4 and CCR5 activates Rho family GTPases that are required for optimal infection of primary CD4+ T cells. Retrovirology *14*, 4. 10.1186/s12977-017-0328-7.

42. Rosa, A., Chande, A., Ziglio, S., De Sanctis, V., Bertorelli, R., Goh, S.L., McCauley, S.M., Nowosielska, A., Antonarakis, S.E., Luban, J., et al. (2015). HIV-1 Nef promotes infection by excluding SERINC5 from virion incorporation. Nature *526*, 212–217. 10.1038/nature15399.

43. Usami, Y., Wu, Y., and Göttlinger, H.G. (2015). SERINC3 and SERINC5 restrict HIV-1 infectivity and are counteracted by Nef. Nature *526*, 218–223. 10.1038/nature15400.

44. Bosso, M., Stürzel, C.M., Kmiec, D., Badarinarayan, S.S., Braun, E., Ito, J., Sato, K., Hahn, B.H., Sparrer, K.M.J., Sauter, D., et al. (2021). An additional NF-κB site allows HIV-1 subtype C to evade restriction by nuclear PYHIN proteins. Cell Rep *36*, 109735. 10.1016/j.celrep.2021.109735.

45. Hotter, D., Bosso, M., Jønsson, K.L., Krapp, C., Stürzel, C.M., Das, A., Littwitz-Salomon, E., Berkhout, B., Russ, A., Wittmann, S., et al. (2019). IFI16 Targets the Transcription Factor Sp1 to Suppress HIV-1 Transcription and Latency Reactivation. Cell Host and Microbe. 10.1016/j.chom.2019.05.002.

46. Lama, J. (2003). The physiological relevance of CD4 receptor down-modulation during HIV infection. Current HIV research *1*, 167–184.

47. Lusic, M., Marini, B., Ali, H., Lucic, B., Luzzati, R., and Giacca, M. (2013). Proximity to PML Nuclear Bodies Regulates HIV-1 Latency in CD4+ T Cells. Cell Host and Microbe *13*, 665–677. 10.1016/j.chom.2013.05.006.

48. Castro-Gonzalez, S., Colomer-Lluch, M., and Serra-Moreno, R. (2018). Barriers for HIV Cure: The Latent Reservoir. AIDS research and human retroviruses *34*, 739–759. 10.1089/AID.2018.0118.

49. Devadas, K., and Dhawan, S. (2006). Hemin activation ameliorates HIV-1 infection via heme oxygenase-1 induction. J Immunol *176*, 4252–4257. 10.4049/jimmunol.176.7.4252.

50. Seu, L., Burt, T.D., Witte, J.S., Martin, J.N., Deeks, S.G., and McCune, J.M. (2012). Variations in the heme oxygenase-1 microsatellite polymorphism are associated with plasma CD14 and viral load in HIV-infected African-Americans. Genes Immun *13*, 258–267. 10.1038/gene.2011.76.

51. Kim, D.-H., Ahn, H.-S., Go, H.-J., Kim, D.-Y., Kim, J.-H., Lee, J.-B., Park, S.-Y., Song, C.-S., Lee, S.-W., Ha, S.-D., et al. (2021). Hemin as a novel candidate for treating COVID-19 via heme oxygenase-1 induction. Sci Rep *11*, 21462. 10.1038/s41598-021-01054-3.

52. Zhang, S., Wang, J., Wang, L., Aliyari, S., and Cheng, G. (2022). SARS-CoV-2 virus NSP14 Impairs NRF2/HMOX1 activation by targeting Sirtuin 1. Cell Mol Immunol *19*, 872–882. 10.1038/s41423-022-00887-w.

53. King, C.R., Liu, Y., Amato, K.A., Schaack, G.A., Mickelson, C., Sanders, A.E., Hu, T., Gupta, S., Langlois, R.A., Smith, J.A., et al. (2023). Pathogen-driven CRISPR screens identify TREX1 as a regulator of DNA self-sensing during influenza virus infection. Cell Host Microbe *31*, 1552-1567.e8. 10.1016/j.chom.2023.08.001.

54. Li, Z., Zhong, L., He, J., Huang, Y., and Zhao, Y. (2021). Development and application of reverse genetic technology for the influenza virus. Virus Genes *57*, 151–163. 10.1007/s11262-020-01822-9.

55. Bosso, M., and Kirchhoff, F. (2020). Emerging Role of PYHIN Proteins as Antiviral Restriction Factors. Viruses *12*, 1464. 10.3390/v12121464.

56. Huérfano, S., Šroller, V., Bruštíková, K., Horníková, L., and Forstová, J. (2022). The Interplay between Viruses and Host DNA Sensors. Viruses *14*, 666. 10.3390/v14040666.

57. Justice, J.L., and Cristea, I.M. (2022). Nuclear antiviral innate responses at the intersection of DNA sensing and DNA repair. Trends Microbiol *30*, 1056–1071. 10.1016/j.tim.2022.05.004.

58. Bravo, J.P.K., Hallmark, T., Naegle, B., Beisel, C.L., Jackson, R.N., and Taylor, D.W. (2023). RNA targeting unleashes indiscriminate nuclease activity of CRISPR–Cas12a2. Nature *613*, 582–587. 10.1038/s41586-022-05560-w.

59. Hotter, D., Sauter, D., and Kirchhoff, F. (2013). Emerging role of the host restriction factor tetherin in viral immune sensing.

60. Bruchez, A., Sha, K., Johnson, J., Chen, L., Stefani, C., McConnell, H., Gaucherand, L., Prins, R., Matreyek, K.A., Hume, A.J., et al. (2020). MHC class II transactivator CIITA

induces cell resistance to Ebola virus and SARS-like coronaviruses. Science *370*, 241–247. 10.1126/science.abb3753.

61. Zhang, Z., Zheng, L., Yu, Y., Wu, J., Yang, F., Xu, Y., Guo, Q., Wu, X., Cao, S., Cao, L., et al. (2020). Involvement of SAMHD1 in dNTP homeostasis and the maintenance of genomic integrity and oncotherapy (Review). Int J Oncol *56*, 879–888. 10.3892/ijo.2020.4988.

62. Henderson, S., and Fenton, T. (2015). APOBEC3 genes: retroviral restriction factors to cancer drivers. Trends Mol Med *21*, 274–284. 10.1016/j.molmed.2015.02.007.

63. Wang, W.-X., Kyprianou, N., Wang, X., and Nelson, P.T. (2010). Dysregulation of the mitogen granulin in human cancer through the miR-15/107 microRNA gene group. Cancer Res *70*, 9137–9142. 10.1158/0008-5472.CAN-10-1684.

64. Koepke, L., Winter, B., and Sparrer, K.M.J. (2020). An improved method for high-throughput quantification of autophagy. Scientific Reports *10*, 1–20. 10.1038/s41598-020-68607-w.

Figure legends

Fig. 1. Assay principle and proof of concept. a, Outline of the CRISPR/Cas9-based virus-guided discovery approach. Proviral HIV-1 constructs are engineered to contain the gRNAs expression cassette between the *nef* gene and the 3`LTR. To produce virus stocks, HEK293T cells are transfected with libraries of HIV-1 constructs expressing various gRNAs. The resulting swarms of HIV-1 gRNA viruses are passaged every two days in Cas9-expressing cells in the presence or absence of IFN-β. Cells and viral supernatants are harvested every five days and the frequencies of HIV-1 gRNAs are determined by next-generation sequencing. Target genes of gRNAs that are selected and hence are associated with an advantage for viral replication are cloned and examined for their antiviral activity and mechanism. Note that the U6-gRNA-scaffold region is not to scale and just encompasses 351 or 352 base pairs. **b,** Enrichment of HIV-1 NL4-3 expressing gRNAs targeting tetherin and GBP5. The left panel provides a schematic showing tetherin trapping HIV-1 particles at the cell surface and inhibition of furin-mediated processing of the gp160 Env precursor to mature gp120 and gp41. The right panels show the enrichment of the indicated gRNAs at different days post-infection in presence and absence of IFN-β. Relative enrichment was quantified using SYBR green qPCR. Relative frequencies of the gRNAs were measured in triplicates at each timepoint. **c,** Flow cytometric analysis of tetherin and GBP5 in CEM-M7 Cas9 infected with HIV-1 NL4-3 expressing either tetherin_1, GBP5_2 or NT gRNA.

Fig. 2. Selection of HIV-1 U6-CRF-gRNA constructs targeting *GRN* and *CIITA*. a, Scatter plot of individual sgRNA counts in CEM-M7 cells supernatants non-treated (left panel) or treated with IFN- (right panel) 15 days post infection (red outlines) and in the input (blue outlines) versus gene names sorted by fold enrichment. NT and dotted line indicate the occurrence of the first non-targeting control sgRNA. Selected factors are highlighted by colors as indicated. **b,** Volcano plots indicating specific target genes of which the gRNAs are

significantly enriched during passage in CEM-M7 (upper) or SupT1 CCR5 high (lower) Cas9 cells at different days post infection (dpi). Dashes lines indicate p value 0.05 and 2-fold change respectively on Y and X axis and were used to determine significantly selected genes. **c,** Read counts relative to input virus from the MAGeCK analysis showing the enrichment of gRNAs targeting GRN, CIITA, CC2D1B and CEACAM3 in presence or absence of IFN-β in CEM-M7 Cas9 cells. **d**, Correlation between MAGeCK score obtained in independent experiments in CEM-M7 cells. **e,** Venn diagram illustrating the genes of which the gRNAs were enriched in the different conditions (e.g. different cell lines or in presence or absence of IFN-β). Genes were considered enriched when the $-\log_{10}$ of the positive MAGeCK score was 1.5 or higher. GRN is selected from the virus independently from the experimental setup. **f,** Read counts relative to input virus from the MAGeCK analysis showing the enrichment of gRNAs targeting GRN, CIITA, CC2D1B and CEACAM3 in presence or absence of IFN-β in SupT1 CCR5 high Cas9 cells.

Fig. 3. Impact of PGRN and CIITA on HIV-1 replication. a, Expression of cellular factors targeted by gRNAs selected during passage of HIV-1 in CEM-M7 and SupT1 CCR5 high Cas9 cells with or without the indicated IFNs (1000U/ml). Whole-cell lysates were immunoblotted and stained with antibodies against the indicated proteins. **b,** Percentage of eGFP positive cells indicating infected CEM-M7 Cas9 cells at 4 days post infection electroporated with either the NT or GRN gRNA and infected with WT NL4-3. Bars represent the mean of infected cells at 2dpi relative to the control (100%) of three independent experiments, ±SEM, *$p<0.05$, Student´s t-test Welch´s correction, ** $p<0.001$, ***$p<0.0001$ In the lower panel a representative WB showing PGRN KO efficiency. **c,** HEK293T cells were cotransfected with increasing amounts of GRN expression construct and proviral mutants of NL4-3 or CH077 lacking the accessory genes. Each point represents the average of three independent experiments ±SEM. In the lower panel a representative WB indicating expression of Env, p55, p24 and PGRN in virus supernatants or cell lysates. **d,** HEK293T cells were cotransfected with

a luciferase reporter constructs under the control of the HIV-1 LTR and expression constructs for GRN in presence and absence of NL4-3 Tat or a vector control. Bars represent the mean of three independent experiments ±SEM, Student´s t-test Welch´s correction, *p<0.05, ** p<0.001, ***p<0.0001.**e,** HEK293T cells were cotransfected with different amount of GRN expression plasmid with either NL4-3_eGFP, CH077_eGFP or CH058_eGFP. Early infection was measured with Flow cytometry and bars represent the mean fluorescence intensities (MFI) of eGFP in the eGFP+/GRN+ population relative to vector control (100%). Bars represent the mean of three independent experiments ±SEM, Student´s t-test Welch´s correction, *p<0.05, ** p<0.001, ***p<0.0001. **f,** Representative WB and quantification of PGRN KO.in primary $CD4^+$ T cells. Bars represent the mean of three independent experiments ±SD, Student´s t-test Welch´s correction, *p<0.05, ** p<0.001, ***p<0.0001. **g,** $CD4^+$ T cells from 3 to 6 donors were electroporated with either the GRN gRNA or the NT control, infected with the indicated WT HIV-1 strains and infectious virus yields measured from 2 to 6dpi by TZM-bl infection assays. Values represent the mean of three to six experiments normalized to the NT control (100%) ±SEM, Two-way anova Sidak´s multiple comparison, *p<0.05, ** p<0.001, ***p<0.0001.

Fig. 4. Impact of CIITA, CC2D1B and CEACAM3 on HIV-1 replication. a, HEK293T cells were cotransfected with increasing amount of either CIITA, CC2D1B or CEACAM3 expression constructs with and indicated proviral constructs. Values represent the mean of three independent experiments ±SEM, Student´s t-test Welch´s correction, *p<0.05, ** p<0.001, ***p<0.0001. **b-d,** $CD4^+$ T cells from 3 to 4 donors were electroporated with either the gRNA targeting *CIITA*, *CC2D1B*, *CEACAM3* or the NT control, infected with the indicated WT HIV-1 strains and infectious virus yields measured from 2 to 6 dpi by TZM-bl infection assays. Values represent the mean of two to six experiments normalized to the NT control (100%) ±SEM, Two-way anova Sidak´s multiple comparison *p<0.05, ** p<0.001, ***p<0.0001. Examples from primary data are shown in Extended Data Fig. 3. **e,** Percentage of p24 antigen

in the supernatants of $CD4^+$ T cells from three to four donors electroporated with either the gRNA targeting CC2D1B or NT control at 3 days post infection with VSV-G pseudo-typed Δ*env* NL4-3 or CH077. Bars represent the mean of the infectious viral yield at two days post-infection relative to the control (100%) of three to four independent experiments, ±SEM, Student´s t-test Welch´s correction, *p<0.05, ** p<0.001, ***p<0.0001 In the lower panel a representative WB showing CC2D1B KO efficiency.

Fig. 5. gRNAs targeting *HMOX*, *EHMT2*, *CEACAM3* and *RHOA* increase replication fitness of HIV-1 CH077.a, Volcano plots indicating specific target genes of which the gRNAs are enriched during passage in CEM-M7 Cas9 cells at different days post infection (dpi) after passaging of the CH077 TV-NL4-3-CRF-gRNA in presence of IFN-β. Dashes lines indicate p-value 0.05 and 2-fold change respectively on Y and X axis and were used to determine selected genes. **b,** Venn diagram illustrating the genes of which the gRNAs were enriched in the different conditions in presence of IFN-β. Genes were considered enriched when the MAGeCK score was 1.5 or higher. **c,** Read counts relative to input virus from the MAGeCK analysis showing the enrichment of gRNAs targeting *HMOX1* (upper) or *EHMT2* (lower) in presence or absence of IFN-β in CEM-M7 or SupT1-CCR5 Cas9 cells after passaging or the NL4-3 (left) or CH077 (right) library. **d,** Read counts relative to input virus from the MAGeCK analysis showing the enrichment of gRNAs targeting *CEACAM3* after passaging the NL4-3 (left) or CH077 (right) library. **e,** Read counts relative to input virus from the MAGeCK analysis showing the enrichment of gRNAs targeting *RHOA* after passaging the NL4-3 (left) or CH077 (right) library.

Fig. 6. Selection of sgRNAs by HIV-1 U6-CRF-gRNA constructs lacking *nef*. a, Schematic structure of the *nef*-defective HIV-1 TV-NL4-3-CRF-gRNA constructs. **b,** Venn diagram illustrating the genes of which the gRNAs were enriched in presence and absence of Nef. Genes were considered enriched when the MAGeCK score was 1.5 or higher. sgRNAs targeting *GRN*,

HMOX1, EHMT2 and *CIITA* are selected in both conditions. **c,** Volcano plot indicating significant enrichment of sgRNAs target the *SERINC5* coding gene in Δ*nef* kinetics compared to WT kinetic during passage in CEM-M7 at 15 dpi. Dashes lines indicate p value 0.05 and 2-fold change respectively on Y and X axis. **d,** Read counts relative to input virus from the MAGeCK analysis showing the enrichment of gRNAs targeting SERINC5 in Δ*nef* and WT kinetics. **e,** Read counts relative to input virus from the MAGeCK analysis showing comparison between Δ*nef* kinetics and WT kinetic for each gRNA targeting *SERINC5* at 15 dpi. **f-h,** Selection of sgRNAs targeting *IFI16* as described for *SERINC5* in panels c-e, except that in enrichment in CEM-M7 was determined in the presence of IFN-β. **i,** HEK293T cells were cotransfected with increasing amounts of IFI16 expression construct and indicated proviral constructs lacking *nef*. Each point represents the mean of three independent experiments ±SD, Student´s t-test Welch´s correction, *p<0.05, ** p<0.001, ***p<0.0001.

Prelli Bozzo, Laliberté *et al.*

Figure 1

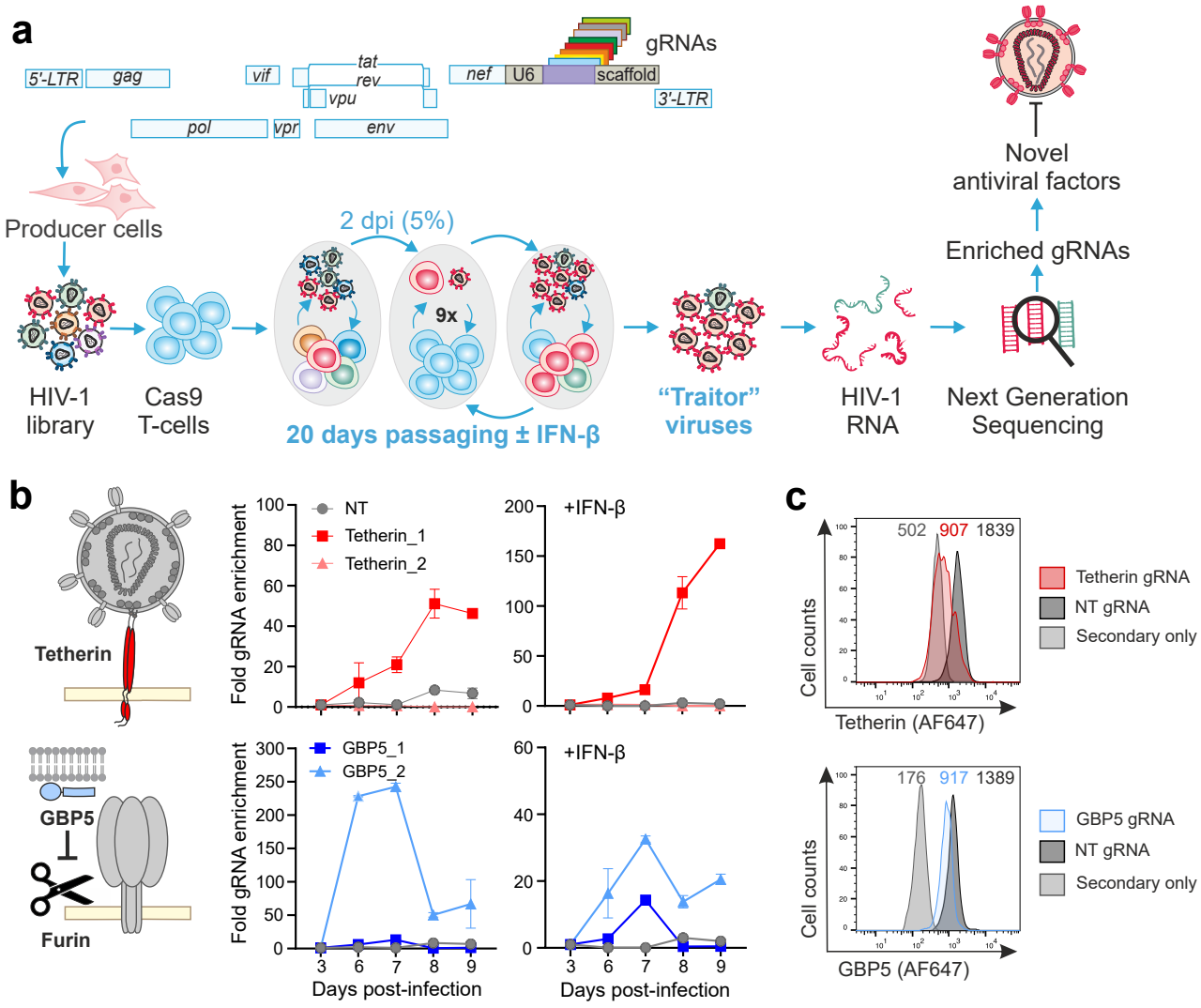

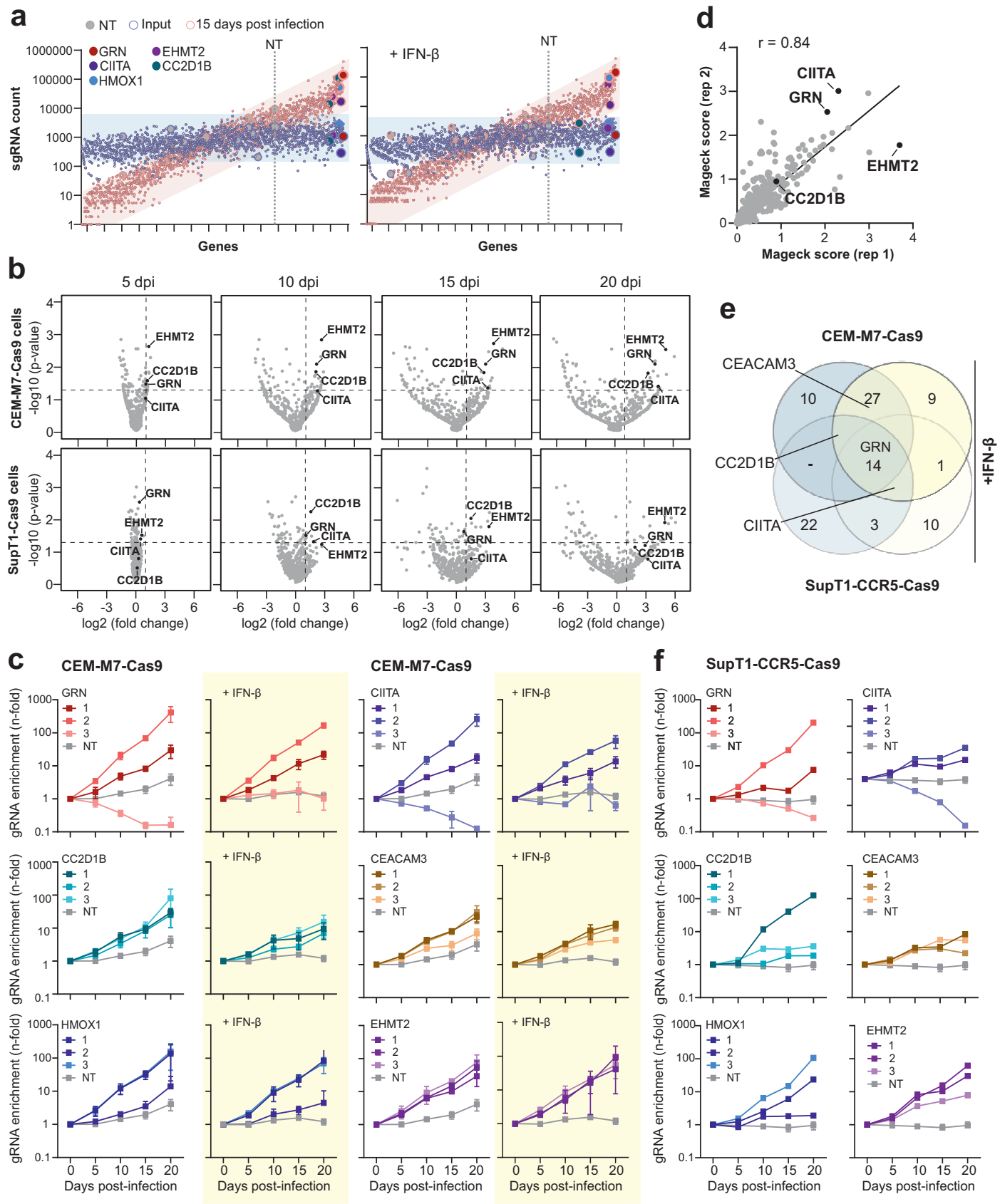

Prelli Bozzo, Laliberté *et al.*

Figure 3

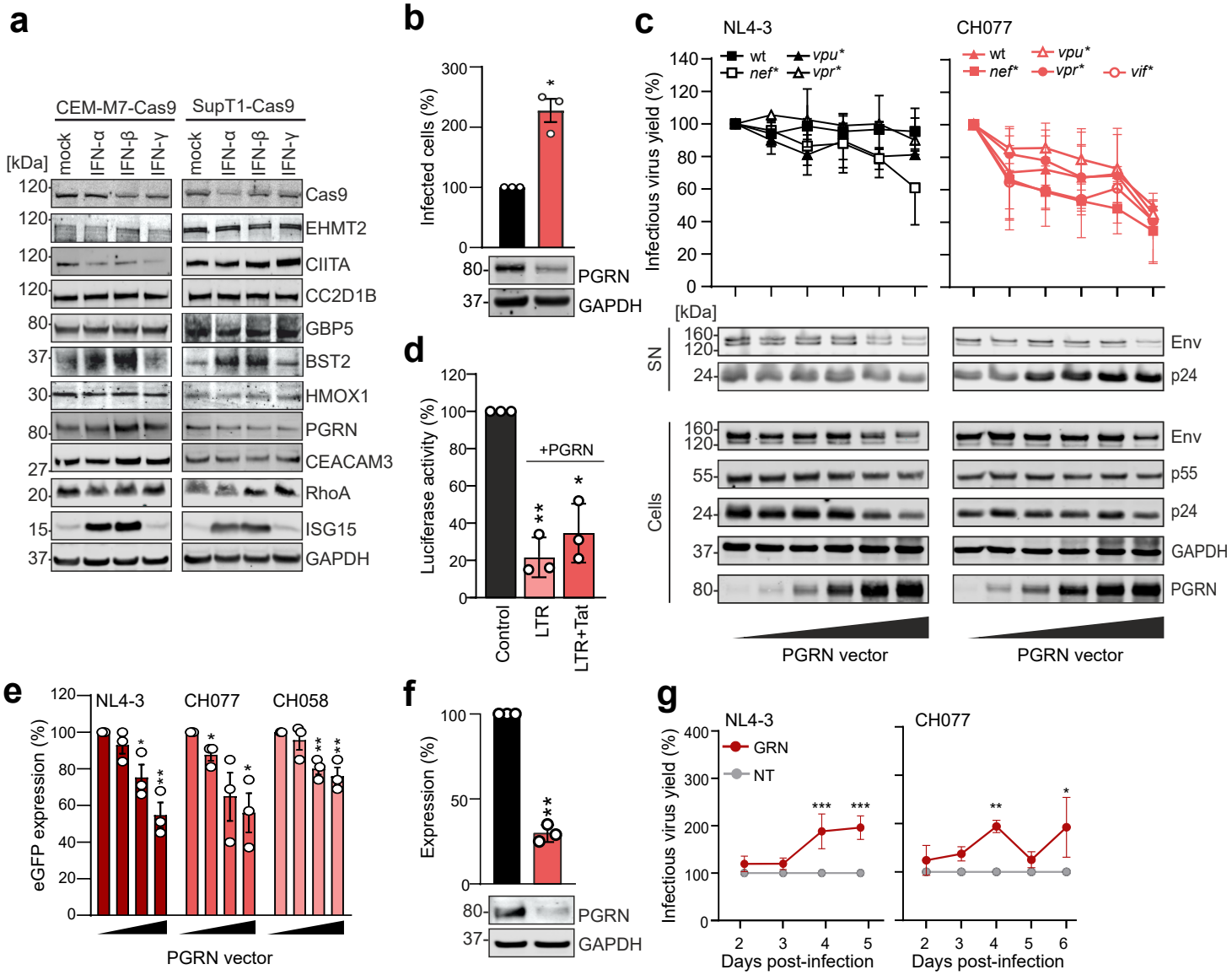

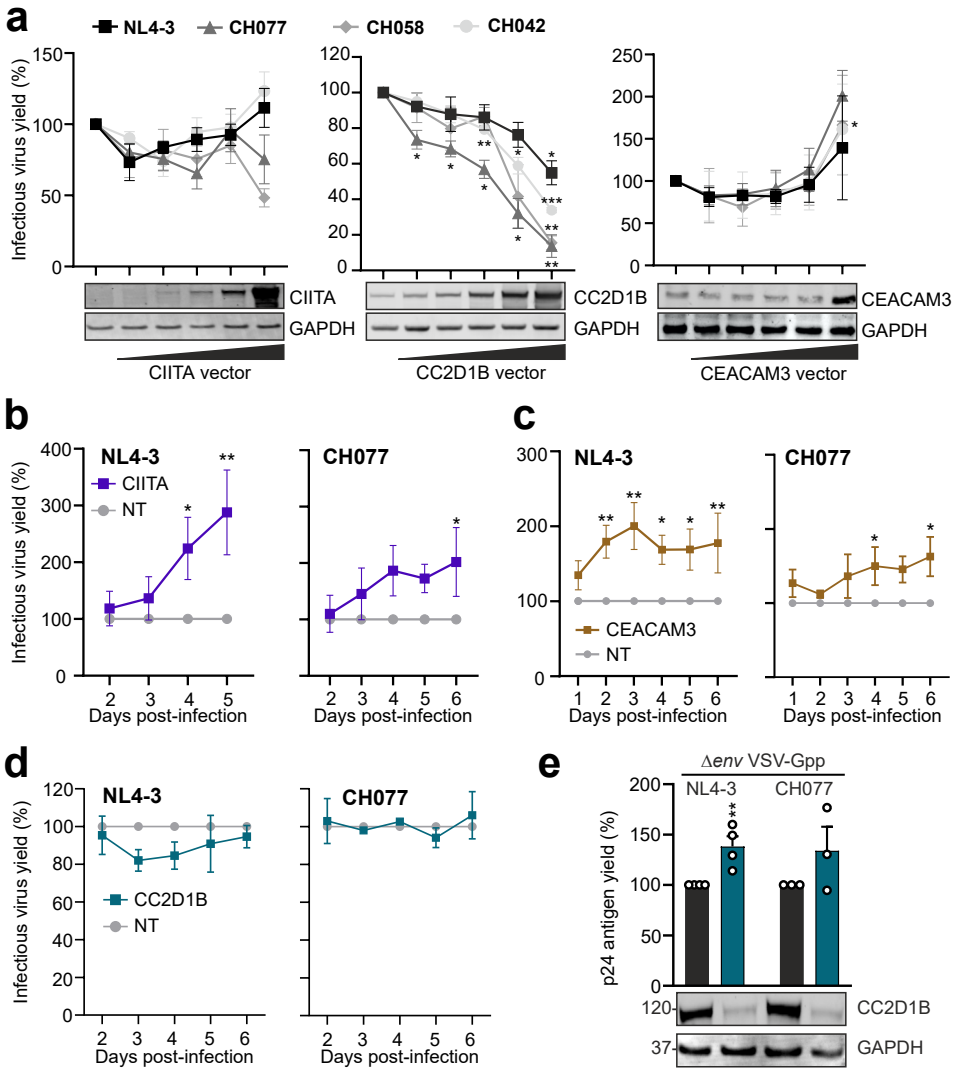

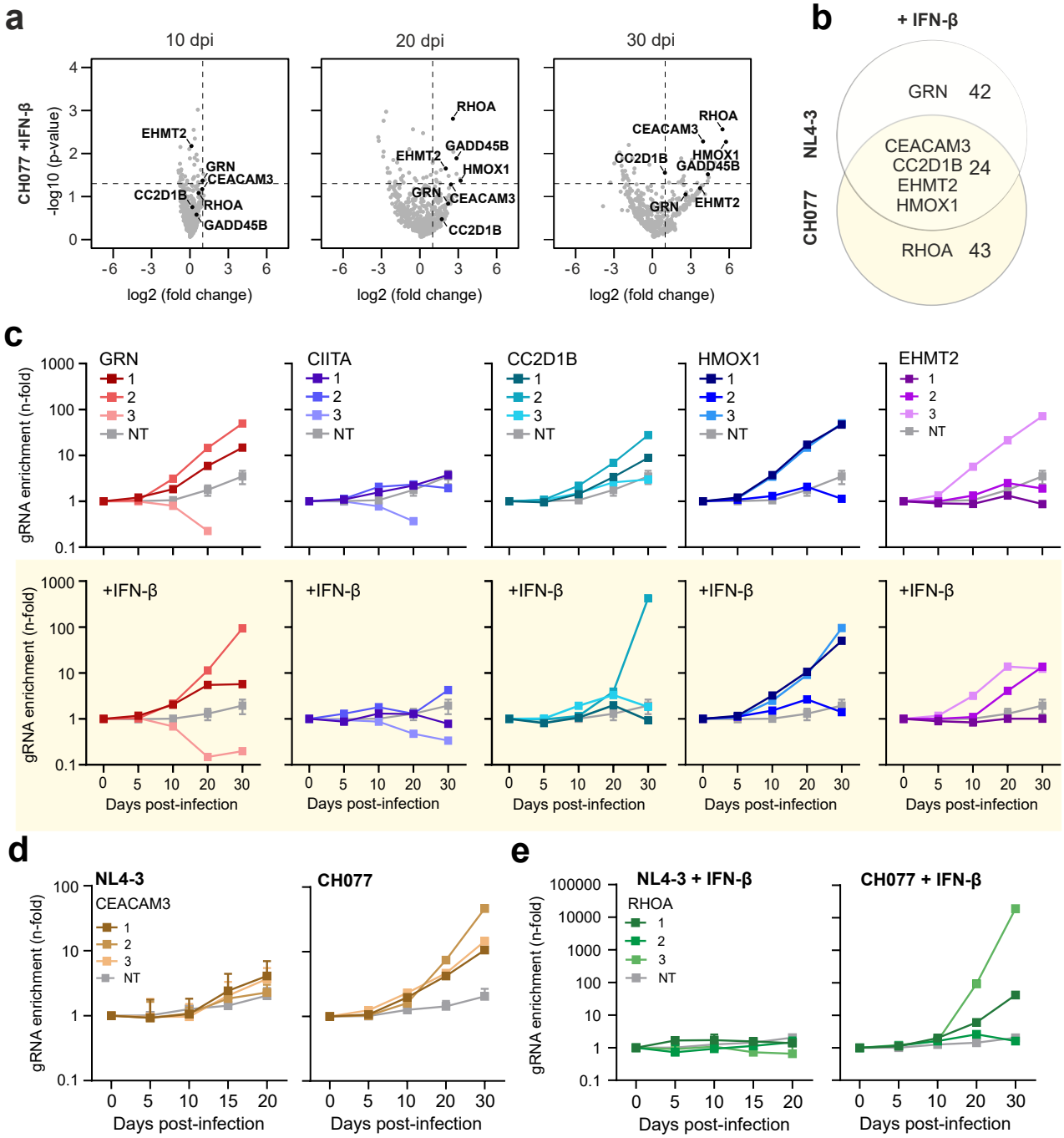

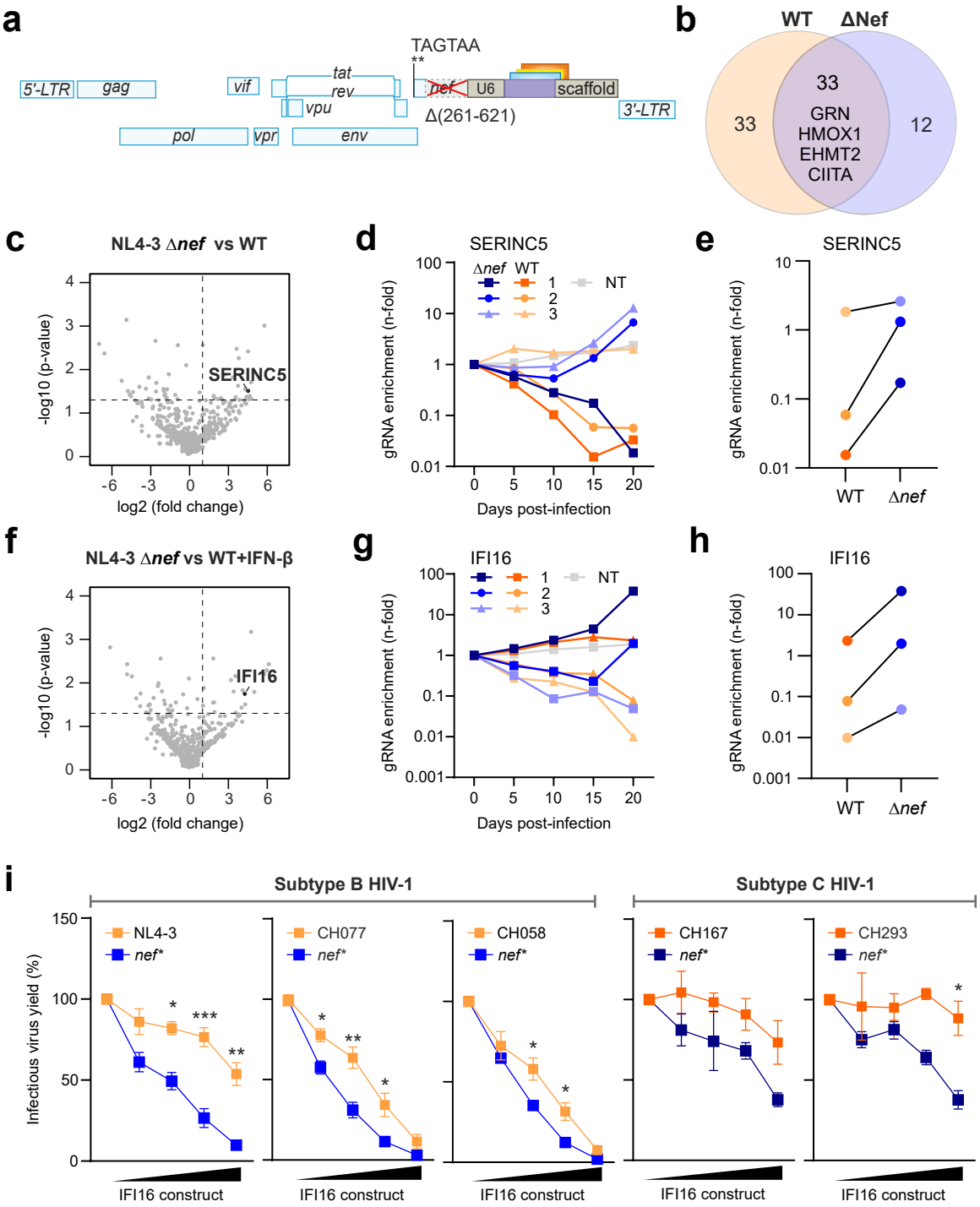

Extended Data of

Traitor-Virus-guided Discovery of novel Antiviral Factors

Caterina Prelli Bozzo[1#], Alexandre Laliberté[1#], Aurora De Luna[1], Chiara Pastorio[1], Kerstin Regensburger[1], Stefan Krebs[2], Alexander Graf[2], Helmut Blum[2], Meta Volcic[1], Konstantin M.J. Sparrer[1*] & Frank Kirchhoff[1*]

[1] Institute of Molecular Virology
Ulm University Medical Center
89081 Ulm, Germany

[2] Laboratory for Functional Genome Analysis
Gene Center, LMU Munich,
81377 Munich, Germany

[#] contributed equally

* Correspondence: Konstantin.Sparrer@uni-ulm.de and Frank.Kirchhoff@uni-ulm.de

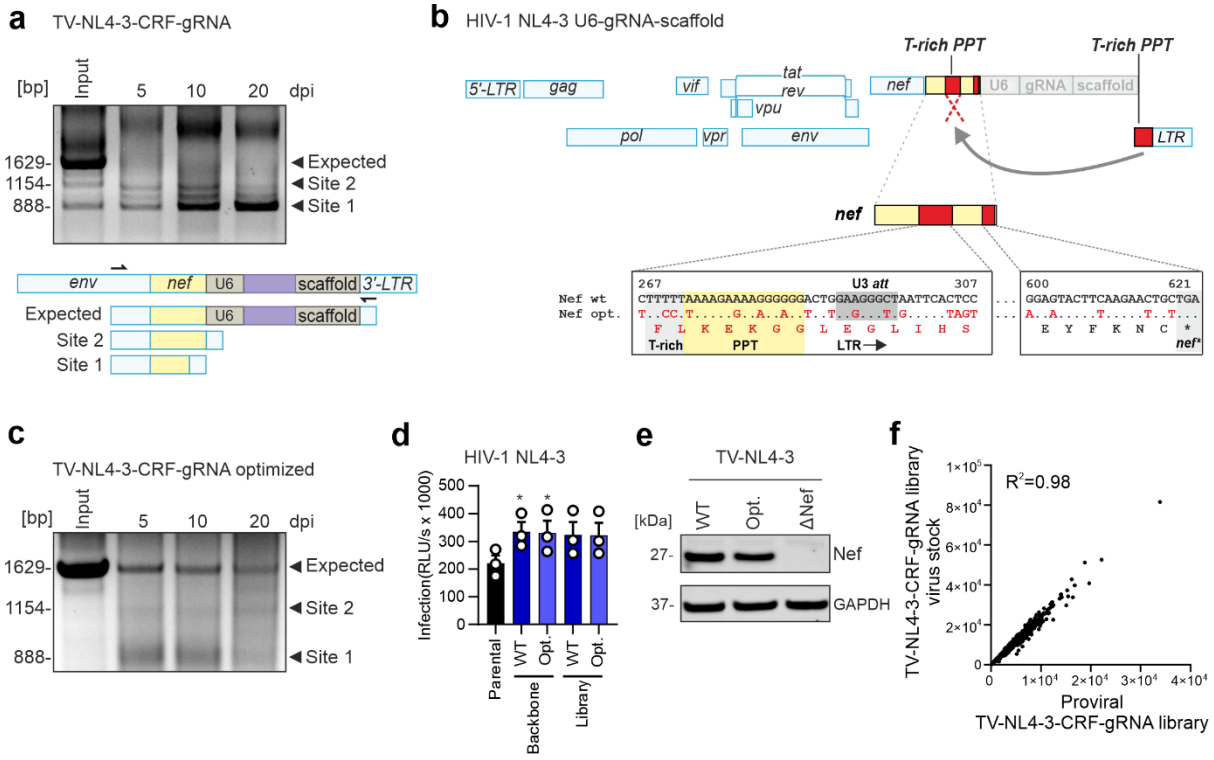

Extended Data Figure 1. Optimization of HIV-1 NL4-3 gRNA construct. a, PCR analysis of the input HIV-1 gRNA stocks and viral variants obtained after the indicated days of passaging. The upper panel shows primary PCR data and the lower panel the position of the primer binding sites and the fragments obtained. **b,** Schematic structure of the HIV-1 genome and modifications at its 3`end to insert the U6-gRNA-scaffold expression cassette. Duplicated T-rich regions, poly-purine tract (PPT) and LTR sequences are highlighted in red. The arrow indicates the major recombination event. Mutations introduced to minimize recombination and the predicted Nef amino acid sequence are indicated. Numbers refer to nucleotide positions in the NL4-3 *nef* gene. **c,** PCR analysis was performed as in panel A but the optimized HIV-1 NL4-3 gRNA construct containing the changes shown in panel B were used for passaging. **d,** HEK293T cells were transfected with the parental HIV-1 NL4-3 construct, the original or optimized derivative containing the U6-gRNA-scaffold cassette or the gRNA library targeting 511 potential antiviral factors. Infectious virus yield was measured using the TZM-bl reporter cell infectivity assay and values were normalized to the infectious virus yield obtained for the parental NL4-3 construct (100%). Bars represent the mean of three independent experiments ±SD, Unpaired T-test Welch´s correction, *p<0.05, ** p<0.001, ***p<0.0001. **e,** Representative Western blot of Nef and GAPDH expression levels in HEK293T cells transfected with the indicated HIV-1 NL4-3 constructs. **f,** NGS results showing the coverage of the HIV-1 NL4-3 gRNA libraries.

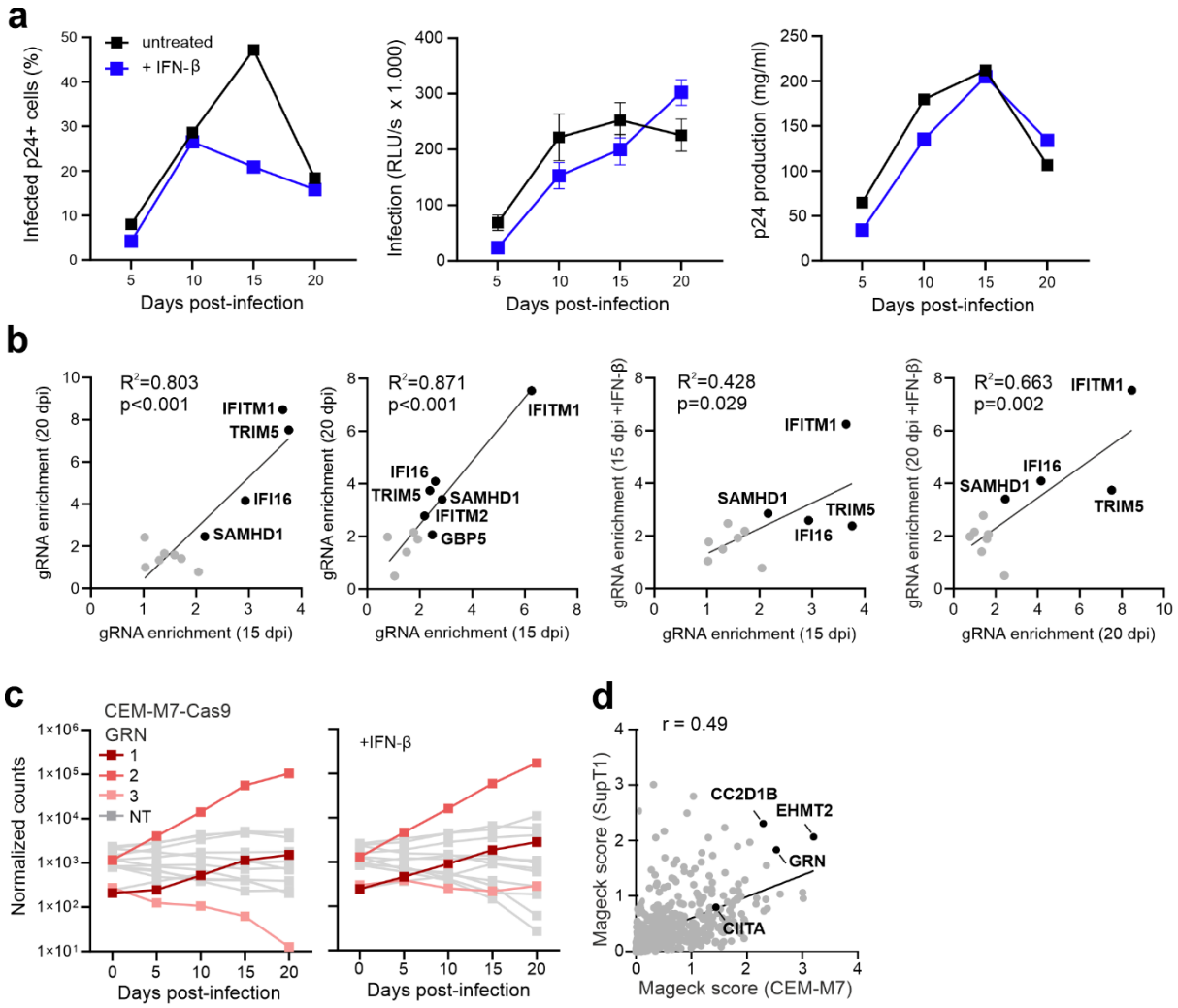

Extended Data Figure 2. Spread and enrichment of HIV-1 CRF-gRNA constructs in cell culture a, Infected cells, infectious virus yields and p24 antigen production in CEM-M7 cells infected with the HIV-1 TC-NL4-3-CRF-gRNA library. Cells were infected and the virus passaged as indicated in Figure 1A. Every five days, the cell cultures were analyzed for the proportion of productively infected (p24+) cells by flow cytometry (left), infectious virus and p24 in the supernatant by TZM-bl infection assay (middle) and p24 antigen ELISA (right), respectively. **b,** Correlation between the enrichment of known RFs at the 15 and 20 day time-points and in the presence or absence of IFN-β in CEM-M7 Cas9 cells. **c,** Absolute counts of the indicated HIV-1 gRNA constructs during passage in CEM-M7 Cas9 cells. **d,** Correlation between MAGeCK score obtained in independent experiments in CEM-M7 vs SupT1 CCR5 high Cas9 cells.

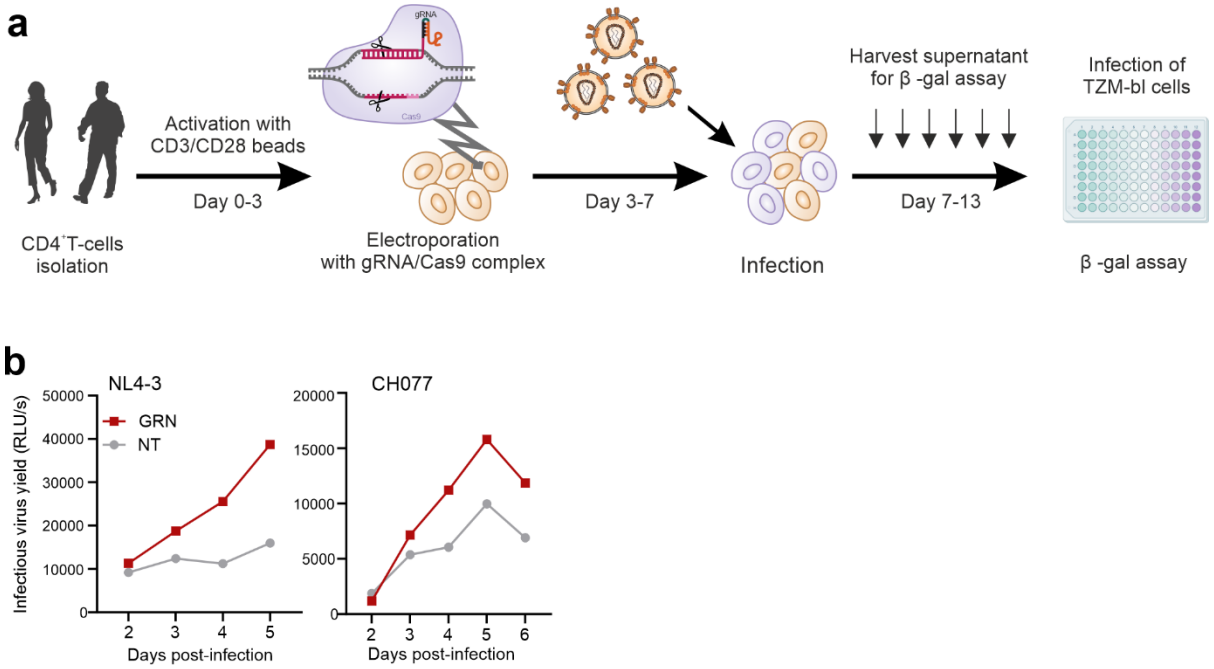

Extended Data Figure 3. Primary data of PGRN and CIITA KO in primary cells. a, Schematic representation of the experimental workflow to KO target genes in primary $CD4^+$ T cells and infect them with WT HIV-.1. **b,** Primary data showing the replication of the indicated WT HIV-1 strains in primary $CD4^+$ T cells electroporated with PGRN, CIITA or NT gRNA.

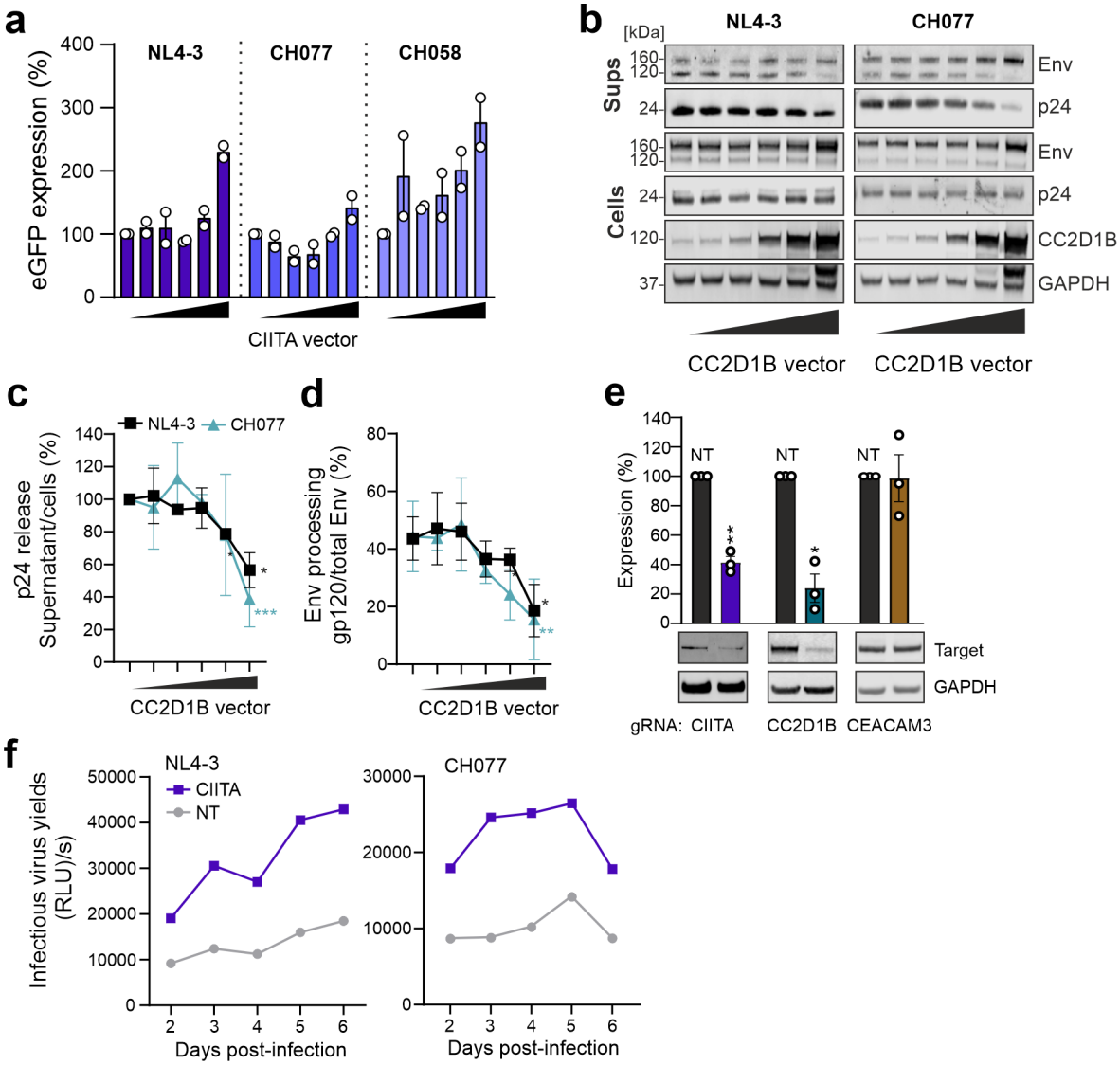

Extended Data Figure 4. Impact of CIITA and CC2D1B on HIV-1 transcription and release. a, HEK293T cells were cotransfected with different amount of CIITA expression plasmid with with either NL4-3_eGFP, CH077_eGFP or CH058_eGFP. Early infection was measured with Flow cytometry and bars represent the mean fluorescence intensities (MFI) of eGFP in the eGFP+/AF647+ population relative to vector control (100%). Bars represent the mean of two independent experiments ±SD. **b,** Representative Western blot showing Env, p24 and CC2D1B in virus containing supernatants or cell lysates of HEN293Ts cotransfected with increasing amounts of CC2D1B and the indicated proviral constructs. **c, d,** Quantification the WB in panel (b) of the p24 release (c) and Env processing (d). Values represent the mean of three independent experiments ±SD, Unpaired T-test Welch´s correction, *p<0.05, ** p<0.001, ***p<0.0001. **e,** Representative western blot and quantification of CIITA, CC2D1B and CEACAM3 expression upon KO.in primary $CD4^+$ T cells. Bars represent the mean of three independent experiments ±SD, Unpaired T-test Welch´s correction, *p<0.05, ** p<0.001, ***p<0.0001. **f,** $CD4^+$ T cells were electroporated with gRNA targeting CIITA or the NT control, infected with the indicated WT HIV-1 strains and infectious virus yields measured from 2 to 6 dpi by TZM-bl infection assays. Shown are representative results.

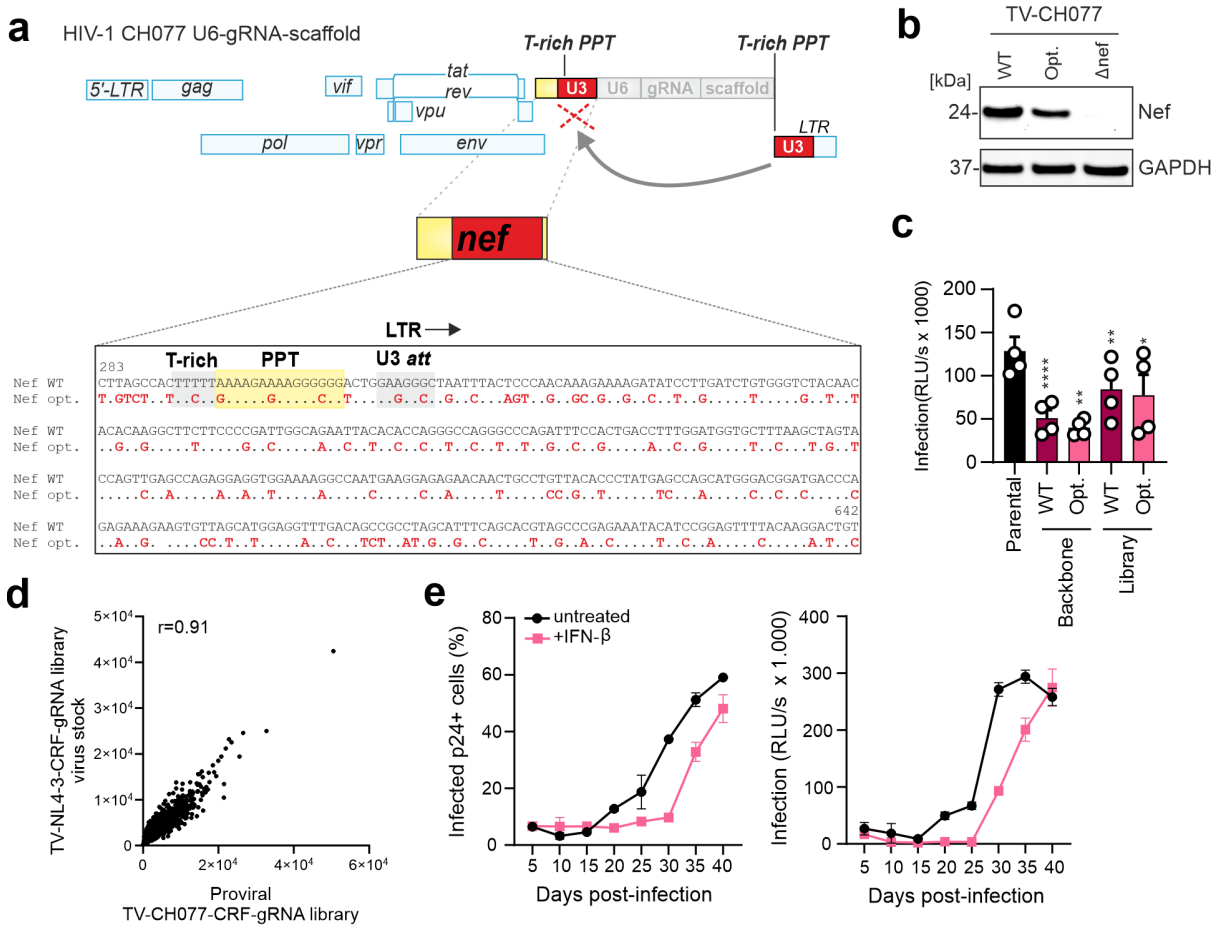

Extended Data Figure 5. Optimization of HIV-1 CH077-3 gRNA constructs. a, Schematic structure of modifications at 3`end to insert the U6-gRNA-scaffold expression cassette. Duplicated T-rich regions, poly-purine tract (PPT) and LTR sequences are highlighted in red. **b,** Nef and GAPDH expression levels in HEK293T cells transfected with the HIV-1 NL4-3 constructs. **c,** Infection rate of parental HIV-1 CH077 construct, the original or optimized containing the U6-gRNA-scaffold cassette or the gRNA library. Bars represent the mean of four independent experiments ±SEM, Unpaired T-test Welch´s correction, *p<0.05, ** p<0.001, ***p<0.0001. **d,** Coverage of the HIV-1 NL4-3 gRNA libraries. **e,** CEM-M7 Cas9 cells infected with the HIV-1 TC-CH077-CRF-gRNA library. the cell cultures were analyzed by flow cytometry (left), infectious virus in the supernatant by TZM-bl infection assay (right), respectively.

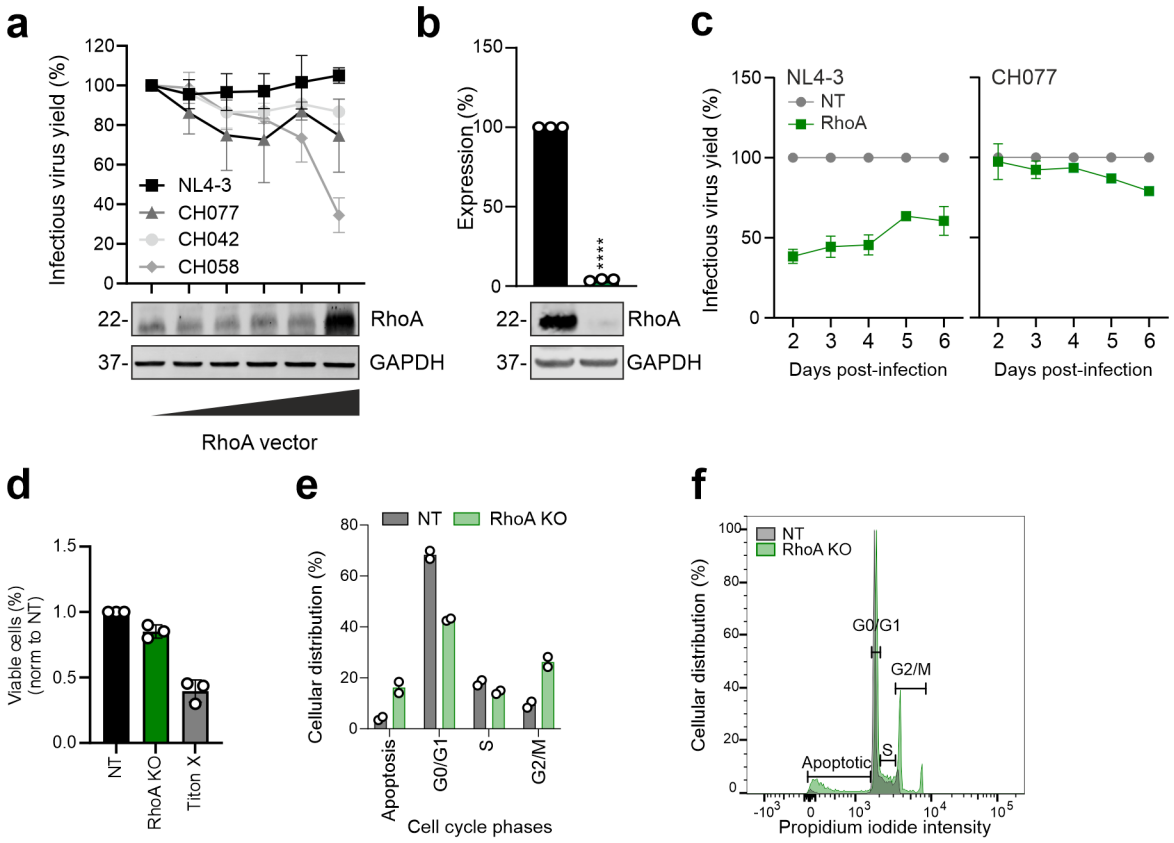

Extended Data Figure 6. RhoA KO impairs HIV-1 replication by inhibiting the cell cycle. **a,** Effect of RhoA overexpression on indicated proviral constructs. Values represent mean of three independent experiments ±SEM. **b,** RhoA expression upon KO.in primary $CD4^+$ T cells. Bars represent the mean of three independent experiments ±SD, Unpaired T-test Welch´s correction, *p<0.05, ** p<0.001, ***p<0.0001. **c,** Effect of RhoA in $CD4^+$ T cells infected with the indicated WT HIV-1 strains. Infectious virus yields measured every day for 5 or 6 days. Values represent the mean of three experiments to the control (100%) ±SEM. **d,** Percentages of viable cells electroporated as described for panel (b). **e,** Percentages of primary $CD4^+$ T cells electroporated with either sgRNA targeting RHOA or the NT control and with Propidium iodide (PI) at different cell cycle phases. Bars represent the mean of two independent experiments ±SD. **f,** Primary representative flow cytometry data showing the gating used in panel (f).

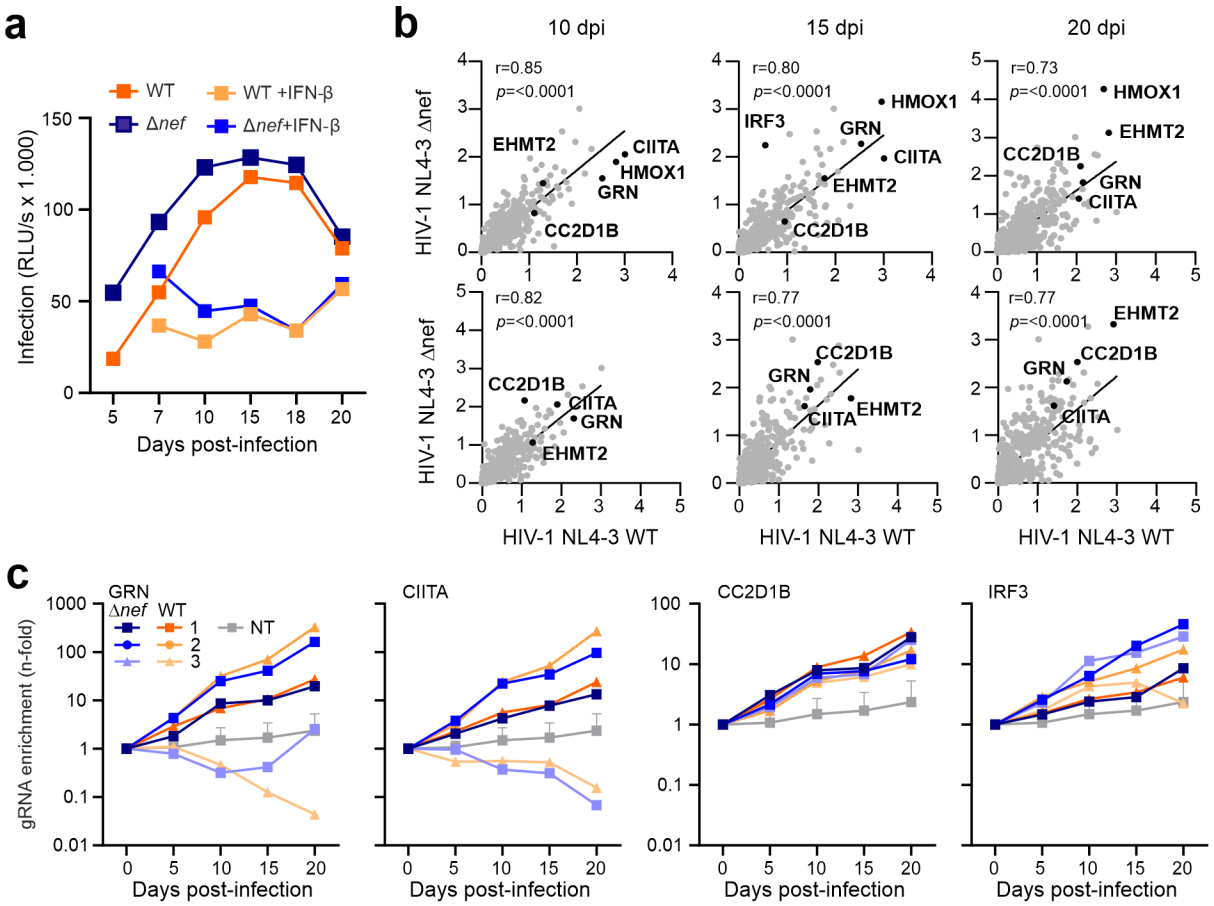

Extended Data Figure 7. Spread and enrichment of HIV-1 CRF-gRNA ΔNef constructs in cell culture. a, Infectious virus yields in CEM-M7 Cas9 cells infected with the TV-NL4-3-CRF-gRNA WT or Δ*nef* library. Cells were infected and the virus passaged as indicated in Figure 1A. Every five days, the cell cultures were analysed for infectious virus in the supernatant by TZM-bl infection. **b,** Correlation between the enrichment of genes at the 10, 15 and 20 day time-points between the WT and Δ*nef* kinetics. **c,** Read counts relative to input virus from the MAGeCK analysis showing the enrichment of gRNAs targeting *GRN*, *CIITA*, *CC2D1B* and *IRF3* in Δ*nef* and WT kinetics.

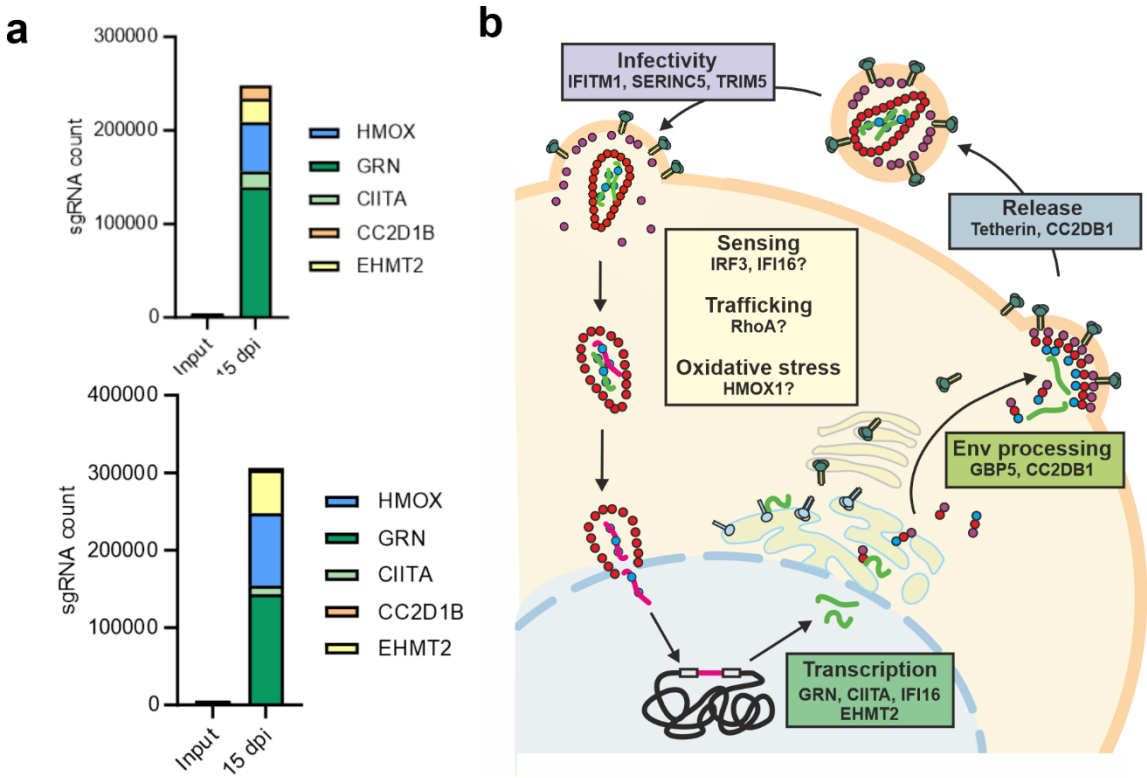

Extended Data Figure 8. Overview on HIV-1-driven selection of sgRNAs and their cellular targets. a, Stacking plot of the enrichment of selected sgRNA counts from input to 15 days post infection of CEM-M7 Cas9 cells, non-treated (upper panel) or treated with IFN-β (lower panel). **b,** Schematic overview on the HIV-1 replication cycles and cellular factors expressed by genes target by sgRNA that became strongly enriched by the TV-driven screening approach. The exact inhibitory mechanisms of some of the highlighted cellular factors remain to be determined.